Published in final edited form as:
Expert Opin Drug Deliv. 2013 May ; 10(5): 573–592. doi:10.1517/17425247.2013.772578.

Ultrasound-mediated drug delivery for cardiovascular disease

Jonathan T Sutton, BS[1], **Kevin J Haworth, PhD**[2,1], **Gail Pyne-Geithman, DPhil**[3,4], and **Christy K Holland, PhD**[1,2,†]

[1]University of Cincinnati, College of Engineering and Applied Science, Biomedical Engineering Program, Cincinnati, OH, USA

[2]University of Cincinnati, College of Medicine, Internal Medicine, Division of Cardiovascular Diseases, 3935 Cardiovascular Center 231 Albert Sabin Way Cincinnati, OH 45267-0586, USA

[3]University of Cincinnati, College of Medicine, Department of Neurosurgery and the University of Cincinnati Neuroscience Institute, Cincinnati, OH, USA

[4]Mayfield Clinic, Cincinnati, OH, USA

Abstract

Introduction—Ultrasound (US) has been developed as both a valuable diagnostic tool and a potent promoter of beneficial tissue bioeffects for the treatment of cardiovascular disease. These effects can be mediated by mechanical oscillations of circulating microbubbles, or US contrast agents, which may also encapsulate and shield a therapeutic agent in the bloodstream. Oscillating microbubbles can create stresses directly on nearby tissue or induce fluid effects that effect drug penetration into vascular tissue, lyse thrombi or direct drugs to optimal locations for delivery.

Areas covered—The present review summarizes investigations that have provided evidence for US-mediated drug delivery as a potent method to deliver therapeutics to diseased tissue for cardiovascular treatment. In particular, the focus will be on investigations of specific aspects relating to US-mediated drug delivery, such as delivery vehicles, drug transport routes, biochemical mechanisms and molecular targeting strategies.

Expert opinion—These investigations have spurred continued research into alternative therapeutic applications, such as bioactive gas delivery and new US technologies. Successful implementation of US-mediated drug delivery has the potential to change the way many drugs are administered systemically, resulting in more effective and economical therapeutics, and less-invasive treatments.

†Author for correspondence: University of Cincinnati, College of Medicine, Internal Medicine, Division of Cardiovascular Diseases, and Biomedical Engineering Program, Cincinnati, OH, USA, Tel: +1 5135585675; Fax: +1 5135586102; christy.holland@uc.edu.

Declaration of interest
Grant funding from NIH R01 NS047603; NIH R01 HL059586; NIH R01 HL74002; NIH F32 HL104916 supported the coauthors during the preparation of this manuscript.

Keywords

cavitation; drug targeting; endothelium; image-guided drug delivery; microstreaming; sonoporation; sonothrombolysis; theragnostic agents; ultrasound bioeffects; ultrasound-enhanced drug delivery

1. Introduction

1.1 Drug delivery for cardiovascular disease

The barrier between the bloodstream and vascular tissue presents a significant challenge to extracorporeal drug delivery. Macromolecules can accumulate on the luminal side of this barrier if appropriate ligands exist to facilitate affinity. Once bound, transport into the local tissue bed occurs if the body's natural mechanisms permit permeability of the endothelium and other vascular barriers [1,2]. Pharmacokinetic modeling, coupled with the development of targeted pharmaceuticals, has improved the specificity and efficacy of therapeutics. However, sensitizing the endothelium to increase local permeability remains an area of active research to improve cardiovascular drug delivery [3].

Methods to direct drug delivery to pathologic cardiovascular tissue are under development. Atherosclerosis, an intensively studied cardiovascular pathology, is characterized by the build-up of lipids, cholesterol and other substances in arterial walls and the formation of plaques [4]. These plaques elicit an immune response [5] and become unstable, shedding fatty deposits and calcified matter into the lumen [6]. The plaque fragments subsequently occlude downstream small-diameter vessels, or become nuclei for thrombi, leading to myocardial infarction, pulmonary thromboembolism or ischemic stroke [7,8].

The treatment of atherosclerosis and other cardiovascular diseases, such as congenital heart disease, rheumatic heart disease, cardiomyopathy and peripheral vascular disease, is limited by the inability to deliver therapeutics across the endothelium safely and effectively [9]. For example, peroxisome proliferator-activated receptor (PPAR) agonists, such as rosiglitazone, have been proposed as a pharmaceutical approach to arrest atheroma by reducing macrophage infiltration into atherosclerotic lesions [10]. However, despite effective *in vitro* activity, rosiglitazone is cytotoxic to healthy cardiovascular tissue and can induce fluid retention, heart failure and further endothelial dysfunction [11]. More effective targeting and delivery methods for rosiglitazone would simultaneously improve efficacy and specificity. Other promising strategies for treating cardiovascular disease include stem cells for repair of ischemic myometrium and valve damage [12]; macromolecular-assisted, thiomer-mediated approaches [13]; nanoparticle-assisted therapies [14,15] and microRNA-mediated gene expression modulation therapy [16]. This review will focus on strategies and mechanisms of ultrasound (US)-mediated cardiovascular drug delivery. Development of effective targeting and delivery methods for the treatment of cardiovascular disease would lead to a paradigm shift in the development of more effective, more economical and less-invasive treatments for many types of cardiovascular pathologies.

1.2 US technology for therapeutic delivery and monitoring

US has been developed as a diagnostic tool to interrogate the acoustic properties of tissue. More recently, therapeutic US has been developed to elicit beneficial bioeffects. When US interacts with stabilized gas bodies, such as echo contrast agents, a localized breach in the endothelial barrier can be triggered [17]. Specific mechanisms mediating this response are actively under study. In addition, theragnostic agents –containing both gas and drugs – are under development; US activates the gas bubble and causes the release of a therapeutic payload [18]. Interaction of US with the gas can also transduce mechanical energy to local tissue, which elicits a biochemical response [19].

The design of therapy-loaded microbubbles targeting cardiovascular tissue is provided in excellent reviews by Lindner [20], Liu *et al.* [21] and Laing and McPherson [14]. Laing and McPherson explored the use of liposomes as targeted therapeutic delivery vesicles [14]. Bekeredjian *et al.* outlined the role of US contrast agent destruction as a particular mechanism for gene and drug delivery [22]. Bull provided descriptions of microbubble designs and the fluid microdynamics induced by oscillating microbubbles [23]. Several relevant reviews on techniques for targeting drug-loaded vesicles to the endothelium have also been published [24–26]. This review focuses on US-mediated drug delivery for the treatment of cardiovascular disease, both updating and expanding the aforementioned reviews and focusing on treatment of cardiovascular diseases. The complex interaction of US with microbubbles, including the gently effervescent activity of stable cavitation and the more violent volume pulsations of inertial cavitation are discussed. This focus allows for a detailed discussion of tissue-specific targeting techniques, drug-loaded vesicle design and both physical and biochemical drug delivery pathways.

Acoustic cavitation is the formation and collapse of gaseous and vapor bubbles in a liquid due to an acoustic pressure field [27–41]. Cavitation is generally classified into two types: stable cavitation, which results in acoustic emissions at sub-harmonics of the fundamental frequency and associated ultra-harmonics, and inertial cavitation, which is characterized by broadband acoustic emissions. When a bubble oscillates non-linearly about its equilibrium radius, the radiated pressure wave may include subharmonic content [41–43]. Broadband emissions are generated when bubbles undergo large radial oscillations and collapse violently [34,37]. This type of bubble motion is dominated by the inertia of the surrounding fluid, hence the label ‘inertial’ cavitation. Stable cavitation can induce bubble-associated microstreaming [44,45] and inertial cavitation can cause microjetting and pitting on solid surfaces [46–48]. Exploiting the acoustic impedance mismatch between microbubbles and blood, acoustic radiation force on microbubbles [49,50] has been used to push drug-loaded agents in the bloodstream toward the endothelium for improved local deposition of the drug [51,52]. Similarly, acoustic streaming – a steady fluid flow caused by an acoustic field – can increase mass transport of a therapeutic [53–55].

Acoustic cavitation has been shown to mediate many therapeutic US applications, including drug and gene release and delivery [56–65], and sonothrombolysis [66–70]. Passive and active cavitation detection techniques have been developed to monitor acoustic cavitation [71,72]. Passive schemes employ a transducer that listens passively (i.e., no transmit) to

emissions from acoustically activated microbubbles. More recently, multiple-element arrays have been developed to allow for spatial resolution of bubble activity over a large area [72–76]. Active subharmonic imaging techniques for bubble detection using US arrays have also been implemented [77–79].

2. Barriers to drug delivery

Many factors hinder the penetration of therapeutics from the vascular lumen into an arterial tissue bed, including blood flow, luminal concentration of drug, barrier permeability, pressure-induced convection and intracellular transport rates [80–82]. The specific contributions of each factor within large vessels have been investigated using analytical models specifically developed to describe the transport of tracers into vascular tissue. Penn *et al.* used one such model to describe the *in vivo* penetration of horseradish peroxidase into the tunica of hypertensive rats by treating the arterial bed as a system containing four compartments: the vascular lumen, the tunica intima, the tunica media and the tunica adventitia [82]. Though the endothelium was the dominant barrier to penetration, the internal elastic lamina (IEL) was responsible for up to 25% of penetration resistance. Another study by Penn *et al.* [83] showed that once the endothelial permeability exceeded a threshold, drug accumulated in the intima due to preferential pressure-driven convection. Analytical models of drug delivery are important due to their ability to describe the degree to which individual vascular properties contribute to vascular drug delivery.

The vascular endothelial barrier differs among organ types depending on the function and level of control required for optimal performance. Appreciable differences have been found in structure, signaling control, selectivity and permeability [84]. The vascular endothelial barrier function and integrity can be compromised in many ways, such as bacterial toxins, oxidative stress, ischemia, immune function and dysfunction and vasculopathy as well as cancerous changes [85–89]. Increased understanding of these disease processes not only helps develop theragnostic strategies, but also gives insight into the normal function of the vascular endothelium, which can be manipulated for drug delivery.

Most research effort directed toward drug delivery from the lumen into the tissue bed has been, and continues to be, focused on the blood–brain barrier (BBB). This bias is largely due to relatively recent understanding of the pathophysiology of many neurological diseases and the enormous potential benefit of effective therapeutic delivery. The BBB is a highly selective and tightly regulated endothelial barrier. A complex network of intercellular proteins forms a tight junction. Selective molecular passage is achieved by size exclusion. These proteins are coupled to intracellular structural and signaling proteins within the endothelial cells. Tight junction proteins are in contact with adjacent astrocytic endfeet, conferring a higher level of control and providing avenues for modulation. There is a large body of excellent literature describing this unique barrier [90], the challenges it presents [91], and the approaches to drug delivery currently under investigation [92].

Outside of the brain, transendothelial transport is less stringently regulated, but remains a significant barrier to drug delivery. Within the cardiovascular system, one may encounter endothelial barriers in conductance vessels, capillaries and neovascular tissue (e.g., tumors,

ischemic damage) [93,94]. Aside from differences in interaction with and regulation of vascular smooth muscle [95], variations in barrier structure and function can be discerned [96]. Conductance vessels, such as aorta, pulmonary and coronary arteries, typically possess robust endothelial layers that regenerate quickly after trauma. Also, when healthy, these cells are resistant to shear stress and oxidative damage necessary in a high-pressure, high-flow elastic system. Conductance vessel endothelial function is closely coupled to vascular regulation, monitoring oxygen and substrate levels and providing feedback to the smooth muscle via intrinsic relaxation agents (nitric oxide, bradykinin) or contractile agents (adrenergic β_1-receptor agonists) to adjust bulk flow.

Cardiac microvascular endothelium is a unique barrier that also communicates with neuronal cells to synchronize and regulate heart rate and blood flow [97]. Accordingly, the microvascular endothelium is tightly controlled specifically with respect to electrochemical gradients and ion flow to preserve cardiac neurovascular coupling [98]. Disruption of this barrier could affect normal cardiac function and must be borne in mind when manipulating tight junction proteins in the heart.

Vessels formed during tumorigenesis, as well as in neovascularization of ischemic myometrium, tend to be tortuous and thin-walled. The endothelial layer is easily damaged, and not well regulated [89,94]. Thus, the vascularization of tumors is characterized as *leaky*, a condition often promulgated by tumor cells to foster further pathological angiogenesis serving the tumor [99]. This phenomenon is both a useful avenue for somewhat specific drug delivery to the tumor tissue, and a target for reduction – by drugs or radiation – to starve the tumor [100].

3. Vehicles for enhanced drug delivery

The prospect of controlling drug concentrations within the vascular system by developing responsive physiological systems was outlined in 1986 by Kost and Langer [101]. Since then, US has been established as an effective external trigger for enhanced drug delivery by acoustically agitating vesicles containing encapsulated gas. Several vascular drug delivery vehicles have been proposed to encapsulate therapeutics, such as nanogels [102,103], micelles [104,105] and perfluorocarbon droplet emulsions [106–108]. Drugs and bioactive gases have also been encapsulated in nanometer and micron-sized echogenic liposomes [109–114]. To be an effective vehicle, the agent must maintain stability *in vivo* while protecting the drug against endogenous agents. Second, the payload should be released at an optimal time and location. Table 1 highlights a few drug delivery vehicles being investigated for cardiovascular therapy, and their associated drug encapsulation characteristics.

Liposomal dispersions effectively encapsulate therapeutics [115] and have been granted the Food and Drug Administration (FDA) approval for clinical use to treat cancer and meningitis [111]. Liposomes either encapsulate the drug within the hydrophilic core or the hydrophobic bilayer [116], depending on the molecular structure of the drug. Amphiphilic macromolecules, such as proteins, intercalate within the lipid bilayer, exposing moieties to the extraliposomal space, while shielding other moieties internally. Gases stabilized by a lipid monolayer can also be encapsulated within these vesicles, rendering them echogenic

and more physically responsive to US. Amphiphilic copolymer micelles, which encapsulate drugs within hydrophobic micellar cores or hydrophobic shells, have also been investigated as drug vesicles [117].

Coating the drug delivery agent with biochemically inert substances can effect additional stability against immunogenic or enzymatic degradation that narrow the window of time for drug delivery. Effective drug shielding and increased solubility have been achieved through the use of cyclodextrins [118], which are supramolecular structures capable of forming inclusion complexes with drug molecules. The hydrophilic outer surface of cyclodextrin produces sufficient solubility in aqueous media, yet its interior binding region is hydrophobic, allowing for efficient encapsulation of insoluble organic compounds [111]. Covalent coating with ethylene glycol, or 'PEGylation', decreases a drug's kidney excretion rate, improves solubility and mitigates immunogenicity [119]. Together, these techniques permit the encapsulation of therapeutics that would otherwise be unavailable for use systemically, thus broadening the potential scope of US-mediated drug delivery for treatment of cardiovascular disease.

US-triggered drug release from the vesicle can occur via a variety of mechanisms. Acoustic cavitation is hypothesized to expel the contents of the vesicle within diseased portions of the vasculature, enhancing the therapeutic index and mitigating non-specific cytotoxicity. Gas-encapsulating liposomes are particularly suited for US-triggered release because the cavitation nucleation site is built into the vesicle [114]. Gas-free liposomes have also been shown to release their contents during acoustic cavitation [120]. Alternatively, thermally sensitive liposomes and copolymer micelles release their contents when exposed to hyperthermia in tumor tissue or thermal deposition of US energy [121,122].

4. Tissue targets for US-mediated cardiovascular drug delivery

US can exert direct effects on tissue to enhance cardiovascular drug uptake. These mechanical effects can promote beneficial bioeffects by augmenting the body's natural mechanisms, as in the case of sonothrombolysis [72], or by creating new delivery pathways, as in the case of sonoporation where US induces pore formation in the cellular membrane [123,124]. US is capable of facilitating delivery of bioactive macromolecules, gases and cell nuclear material to a variety of vascular tissue and cell types, such as thrombus [69,125], endothelial cells [126], smooth muscle cells [112] and cellular nuclei [127]. Table 2 highlights some of these investigations.

US-mediated drug delivery to these different tissue targets could involve disparate mechanisms and transport routes, which depend on specific biochemical responses to US. For example, acoustically active, drug-loaded vesicles can become tethered to the endothelial membrane via a vascular ligand [128]. Thereupon, vesicles extravasate i) *paracellularly*, through the breakdown of tight junction proteins [129], ii) *intracellularly* by endocytosis [130] or iii) through *sonoporation* [124]. Recent attempts to manipulate the elastic properties of drug-loaded vesicles have rendered their adhesion to activated endothelium in a similar way to immunoreactive leukocytes [128]. Alternatively, drug delivery to intraluminal thrombi is accelerated by US in a similar fashion to that of blood

flow around and through a clot. The fluid dynamics at the surface of a thrombus replenishes fibrinolytic proteins within the clot [131], while also removing fibrin degradation products [132]. US-mediated drug delivery seeks to promote these processes for the sake of delivering therapeutics to diseased tissue. These pathways, and the hypothesized mechanisms by which US could facilitate their manifestation are depicted in Figures 1, 2 and 3 and discussed sequentially below.

4.1 US-mediated cellular delivery

Currently, a significant body of cardiovascular drug delivery work focuses on US-mediated drug delivery to individual cells. These *in vitro* investigations explore two important interactions vital to drug delivery: i) drug transfer dynamics from a delivery vesicle to a cell and ii) mechanical interactions between cells and oscillating bubbles. Acoustic pressure amplitude, bubble concentration and the proximity of bubbles to cells [133], all play a role in drug delivery efficiency.

Hamster ovary cells exposed to pulsed US exhibited increased uptake of fluorescein isothiocyanate (FITC)-dextran, a fluorescent macromolecule unable to diffuse across plasma membranes [134]. Furthermore, the cells promoted the expression of luciferase plasmids added to the extracellular serum. At higher acoustic pressures (> 0.3 MPa), cells were unable to repair pores in the local membrane caused by acoustic cavitation, resulting in lysis and loss of viability. Mehier-Humbert *et al.* further investigated the extent of pore formation in a study examining the dependence of tracer size on sonoporative transport. Particles of increasing size up to 37 nm in diameter were able to penetrate the plasma membrane in the presence of phospholipid microbubbles exposed to US (0.57 MPa; 1.15 MHz) [135].

The degree of sonoporation, whether ‘reparable’ or ‘lethal’, is also dependent on bubble-to-cell separation. In a flagship study on sonoporation, Ward *et al.* described a non-linear increase in lethal sonoporation as the theoretical bubble-to-cell spacing decreased from 60 μm to below 20 μm for Optison™ microbubbles [136]. The authors posited that acoustic cavitation was responsible for this bioeffect. Based on the published acoustic parameters and experimental setup, recent cavitation simulations support this assertion, predicting that Optison™ microbubbles would nucleate both stable and inertial cavitation [41].

4.2 Mechanisms of cellular delivery

Acoustic cavitation has been the prime emphasis of US-mediated drug delivery, especially for delivery of drugs into cells. When a microbubble experiences an acoustic pressure wave near a biological membrane, bubble oscillations provoke desired [124] or deleterious bioeffects [136]. The type of fluid dynamics that result depend on parameters such as the frequency, amplitude and duration of US [137]; the material properties of the microbubble, its shell and the nearby surface [138] and the degree of bubble proximity to that surface [139]. Several studies have investigated microbubble interactions experimentally [66,137] and theoretically [140].

The microjet formation from inertially collapsing microbubbles can create pores mechanically in the plasma membrane [141]. Endocytosis and subsequent transcytosis can

be stimulated through this localized mechanical destruction of the endothelial membrane. Depicted in Figure 3, cavitating microbubbles near a cell membrane can create a pore for increased membrane permeability to macromolecules, genes and extracellular ions, which is repaired by cellular mechanisms within seconds [124,133,142]. Membrane permeability to extracellular ions upregulates endocytosis of perimembranous macromolecules due to the calcium flux into the cell [143]. Upon apical endocytosis, vesicular macromolecules can be expelled into the cytoplasm, or trafficked basolaterally for exocytosis into the intima, completing the transcytosis pathway [144].

The types of microbubble oscillations required to observe these effects have also been investigated. Inertially cavitating microbubbles near a membrane form 1 – 200 nm pores due to localized tensions [145]. These pores are capable of resealing bifunctionally by either rapid phospholipid rearrangement or gradual, exocytosis-mediated membrane tension changes, which restores membrane integrity [124]. Microbubble-induced tissue damage correlates with the mechanical index at high acoustic pressures, evidenced by linear correlations with cell viability and capillary rupture above 0.61 MPa_{neg} [146]. By definition [33], correlation of this bioeffect with the mechanical index further confirms that tissue damage is associated with inertial cavitation. Evidence of these effects at lower acoustic pressures exists as well. Juffermans *et al.* observed calcium influx into rat cardiomyoblast cells with Sonovue® (Bracco Suisse SA; Geneva, Switzerland) microbubbles at a mechanical index of 0.1, which is likely not sufficient to cause inertial cavitation. Interestingly however, when intracellular hydrogen peroxide was not sequestered during the experiment, the extent of calcium influx increased, suggesting a biochemical mechanism at low acoustic pressures [147]. As the acoustic pressure amplitude is increased however, peroxide-dependent bioeffects are attenuated, as evidenced by Lawrie *et al.* (mechanical index 2.0) [57] and Lionetti *et al.* (mechanical index 1.2) [148].

4.3 Delivery to cardiovascular tissue

Investigations of drug delivery to tissue beds shed light on the extent of drug penetration and the risk of deleterious bio-effects. As illustrated in drug delivery studies to individual cells, a fine line exists between desirable cellular bioeffects and irreversible cell damage. Herbst *et al.* exposed atheromatous porcine carotid vessels to intercellular adhesion molecule (ICAM)-targeted echogenic liposomes conjugated to vascular stem cells in the presence of continuous-wave US [149]. Stem cell delivery to the arterial tunics increased significantly within the intima when exposed to US at a peak-to-peak pressure amplitude of 0.15 MPa, but was absent beyond the IEL. In *ex vivo* murine aortas, ICAM-targeted echogenic liposomes extravasated beyond the endothelium in the presence of 1-MHz continuous-wave US but did not extravasate in the absence of US exposure [150]. The spatial distribution of delivery was confined to the intimal layer, with scant penetration beyond the first few elastic laminae. At these modest acoustic pressures, no US-induced tissue damage was observed histologically.

To promote delivery within the tunica media, Laing *et al.* exposed porcine carotid arteries to α-actin-targeted echogenic immunoliposomes (ELIP) labeled with calcein during 1-MHz US exposure at a peak-to-peak pressure amplitude of 0.23 MPa [112]. Considerable calcein

was observed in the tunica intima and adventitia, suggesting a strong contribution from transendothelial and adventitial delivery routes, respectively. Moderate calcein delivery was observed within the intact tunica media, depicting successful localization within smooth muscle cells (Figure 4).

Within descending porcine coronary arteries after balloon angioplasty, Phillips *et al.* observed increased transgene expression beyond the endothelium with intravascular US exposure *in vivo* [151]. The extent of delivery was again localized to the intimal layer, but endothelial desquamation that often accompanies balloon angioplasty was not investigated [152], opening the possibility of direct delivery to intimal cells aided by mechanical 'pushing' from acoustic radiation force. Together, these investigations of US-mediated drug delivery consistently demonstrate that small macromolecules and cells can be safely delivered to the artery wall when circulating microbubbles are exposed to moderate peak-to-peak pressure amplitude (0.15 – 0.5 MPa) US.

Investigations of US-mediated drug delivery to the myocardium consistently demonstrate robust delivery of growth factors and genetic material for therapeutic benefit [22,133,151,153–155]. Traditional techniques to revascularize diseased coronary artery tissue, such as percutaneous, transmyocardial administration of vascular endothelial growth factor (VEGF) can be improved up to eightfold by administering the growth factor with 1-MHz color-Doppler US and microbubbles, as demonstrated by Mukherjee *et al.* [153]. Chen *et al.* delivered plasmid DNA to the rat myocardium using a combination treatment of 1.3-MHz, intermittent US and plasmid-loaded perfluoropentane (PFP) microbubbles, and observed increased expression relative to untreated liver samples. Additionally, these investigators optimized their US exposures to deliver US bursts gated by the cardiac cycle, and demonstrated considerably higher therapeutic delivery compared with a continuously scanned US regime [154].

4.4 US-mediated mechanisms of vascular tissue delivery

The biochemical and mechanical mechanisms that facilitate drug delivery to vascular tissue are consistent with those that occur during sonoporation. At least three postulated pathways of US-induced passage of materials from the luminal to the adventitial side of vascular tissue have been proposed in the literature: i) paracellular widening of interendothelial clefts and tight junctions, ii) free passage through injured endothelial lining and iii) transcytosis via fenestration and channel formation [129]. These mechanisms have been proposed and modeled [156] for the BBB, but are also supported by studies in other tissue beds, including renal [157], prostate [158] and skeletal muscle [159] tissues.

4.4.1 Paracellular transport—Paracellular transport between functional endothelial cells is supported strongly in the drug delivery literature. Microbubble oscillations in small vessels are known to deform neighboring vessel walls mechanically by direct perturbation or fluid motion [160]. When a microbubble oscillates near a vessel wall, its shell is estimated to travel at speeds on the order of 250 m/s [161], either directly perturbing nearby structures or causing local fluid convection, dubbed as microstreaming (Figure 2) [162]. US exposure of intracranial vessels containing microbubbles showed reversible [163] enhancement of

endothelial opening [129], with neither acute nor chronic tissue damage [164–166]. When microbubble oscillation occurs in the cerebral microcirculation, the BBB is disrupted, causing drug extravasation due to breakdown of transmembrane tight junction proteins [167]: claudins, connexins and occludins [168–170]. VEGF is expressed in vascular endothelial cells in response to shear stress, mechanical disruption and response to immune cytokines in the circulation, or adjacent extravascular tissue. Shang *et al.* [171] quantified three tight junction proteins (claudin-5, occludin and ZO-1) at the mRNA and protein level before, during and after a 3-h exposure to 1-MHz US, in the presence or absence of Optison™ microbubbles [172]. The three tight junction components were significantly reduced (compared with control) by 1-MHz US at 3 and 6 h post-exposure. Twelve hours after exposure, however, the protein expression and presence at the blood–tumor barrier had returned to normal levels. Temporary opening of the endothelial junctions via VEGF signaling is known as an intercellular route for molecule transport [1].

4.4.2 Damage-induced transport—The most disruptive mechanism is the passage of molecules through a compromised endothelium. A recent *ex vivo* study [172] demonstrated that aortic smooth muscle exposed to pulsed color-Doppler and Optison™ microbubbles induced loss of receptor-mediated contractility and endothelium-mediated relaxation. Histologically, loss of endothelium and evidence of endothelial cell apoptosis were apparent. These observations were not seen in tissue treated with US but without Optison™. Chen *et al.* performed a series of experiments observing microbubbles oscillating in venules using ultrahigh-speed microscopy [64,160]. When Definity® microbubbles were exposed to short US pulses (2 μs), small microjets were directed away from the nearest surface, causing considerable invagination of the vessel wall and partial endothelial desquamation. Capillary extravasation of cells [173,174], dyes [175] and other particles [176] due to these large-amplitude bubble oscillations has been observed by a number of investigators, supporting its therapeutic potential for triggering localized, reversible [163] endothelial permeability.

4.4.3 Transcytosis—Microbubble cavitation can also provoke drug transport through a vascular endothelial cell. Transcytosis, in the context of drug delivery, consists of the drug being endocytosed at the luminal surface of the endothelial cell membrane, either in a receptor-mediated fashion [177] or by invagination caused by cavitation with US [178]. Subsequent transportation through several intracellular compartments and secretion from the cell at the basolateral aspect [179,180] results in delivery to vascular tissue. Transcytosis is typically an alternative extension of the caveolar, endocytotic pathway [181]. This is a receptor-mediated process, and provides a pathway for targeted drug delivery via receptor-targeted drug vesicles and US-enhanced endocytosis [182].

4.5 Delivery to thrombus

Sonothrombolysis refers to the expedited dissolution of thrombi due to US exposure. This technique has been tested in clinical trials, but evidence to justify its universal use to treat ischemic stroke lacks consensus. The Combined Lysis of Thrombus in Brain Ischemia Using Transcranial Ultrasound and Systemic tPA (CLOTBUST) trial randomly exposed 126 patients with middle cerebral artery occlusions to intravenous recombinant tissue-

plasminogen activator (rt-PA) and 2-MHz transcranial Doppler US and observed significant clinical improvement in 49% of patients, compared with 30% receiving rt-PA alone [183].

Molina *et al.* extended the clinical investigation of sonothrombolysis by implementing multiple IV microbubble infusions with US exposure [184]. Recanalization rates were significantly improved when Levovist®, a contrast agent, was included with rt-PA and conventional transcranial Doppler US. However, these improvements were modest (54.5 vs 41% with rt-PA/US). Numerous investigators offer reasons for the absence of recanalization improvement in some patients, including inconsistent application of acoustic energy [185] and thrombus immunity to rt-PA lysis due to compositional factors [186,187]. Other investigators cite differences between recanalization and reperfusion, a metric that correlates better with clinical outcome [188].

4.6 Mechanisms of drug delivery to thrombus

Early sonothrombolysis investigations demonstrated efficacy in the presence of a fibrinolytic drug, such as rt-PA [189]. Rather than a direct mechanical or thermal mechanism, US affected the rate of plasminogen cleavage by rt-PA, hastening enzymatic fibrinolysis [190]. Datta *et al.* refined this hypothesis by promoting stable cavitation nucleated by an US contrast agent to enhance the penetration of both rt-PA and plasminogen into clots [69]. These results indicate that expedited fibrinolysis occurs due to increased availability of plasminogen binding sites for rt-PA.

5. Drug targeting

Proposed cavitation-based mechanisms of drug delivery rely on the physical forces exerted by oscillating microbubbles. Since the distance over which these forces are exerted – either by direct perturbation from bubble oscillation [123,124] or fluid streaming [191] – is on the order of a bubble diameter, the microbubbles must be in close proximity with their tissue target. In capillary beds, this requirement is generally met due to the small vessel diameters (< 10 μm) relative to micro-bubble size. However, in larger vessels such as the carotid, femoral or peripheral arteries, the relative fraction of microbubbles near the thrombus or endothelium may not be sufficient to provoke a therapeutic response. Thus, many groups have developed targeted delivery vehicles for efficient US-mediated drug delivery. The most common approach is to conjugate the microbubbles with vascular ligands, so that vesicle adherence to the diseased tissue is promoted. Molecularly targeted, acoustically active drug delivery vesicles have been recently investigated for therapeutic application and diagnosis of inflammation, atherosclerosis, angiogenesis, intravascular thrombosis and post-ischemic injury [192]. Several different antibodies conjugated to microbubbles are reported below.

Atherosclerosis and inflammation facilitate the adherence of both anti-ICAM-1 and anti-vascular cell adhesion protein (anti-VCAM-1) conjugated microbubbles to plated cells and vessels [193–195]. The amount of adherence has been found to vary directly with the degree of atherosclerotic plaque formation [193], the number of molecular receptors present or the activation state of endothelial cells [193]. The ability to target effectively depends on the disease state, as demonstrated with early indication of cardiac transplant rejection in rats [196,197], and initial inflammation of atherosclerosis in mice [194].

Another major approach to targeting endothelium is the use of anti-P-selectin conjugated microbubbles. Takalkar *et al.* showed that once anti-P-selectin conjugated microbubbles were adhered to P-selectin coated plates in a parallel plate flow chamber, shear stresses of 34 dyn/cm^2 were necessary to dislodge approximately half of the microbubbles [198]. To improve the probability of initial adherence, Rychak *et al.* [128] pressurized the microbubbles to cause a partial gas loss. This treatment resulted in an excess shell surface area of approximately 30%, allowing the microbubbles to deform from a spherical shape more readily. The deformable microbubbles adhered to the endothelium in the presence of higher sheer stresses than non-deformable microbubbles. Ferrante *et al.* demonstrated an alternative means of improving adherence by conjugating the microbubbles with both anti-P-selectin and anti-VCAM-1 antibodies [199]. They found that the dual-targeted microbubbles adhered almost twice as efficiently in flow chambers compared with microbubbles targeted with either anti-P-selectin or anti-VCAM-1 alone.

Targeting to improve drug delivery to intraluminal thrombi has also been developed. Platelets, which exist in high concentrations on the surface of thrombi, can be targeted by conjugating a glycoprotein (GP) IIb/IIIa receptor inhibitor to the delivery vesicle [200–204]. Investigations implementing this targeting strategy show enhanced thrombolysis in the presence of a thrombolytic and targeted microbubbles exposed to US. Culp *et al*. [200] and Xie *et al.* [201] both demonstrated that GP IIb/IIIa targeted microbubbles exposed to US expedite lysis more than non-targeted microbubbles *in vivo*. Hua *et al.* [202] demonstrated similar results *in vitro* using microbubbles conjugated to a tetrapeptide for targeting activated platelets. Fibrin can be targeted by conjugating an inactive portion of rt-PA to the drug delivery vesicle. Klegerman *et al.* accomplished targeting to thrombus by intercalating the D-phe-L-pro-L-arg-chloromethyl ketone (PPACK) moiety of rt-PA, which exhibits strong fibrin affinity, within the phospholipid bilayer of ELIP [205].

Anti-α-integrins have been used to target microbubbles to neovascularization *in vivo* [206,207]. Of the total microbubble infusion however, only a small fraction adhere to the diseased endothelium. This physical limitation will be shared by all targeted US theragnostic agents. Acoustic radiation force exerts enough force to push non-targeted microbubbles within close proximity of endothelium *in vivo* by causing particle motion along the axis of acoustic propagation [51,208]. When microbubbles were conjugated to targeting antibodies, the concentration of microbubbles along the vascular increased *ex vivo* [209] and *in vivo* [210]. Further, Liu *et al.* showed that acoustic radiation force can significantly increase adhesion in both arteries (using anti-CD34) and the microvasculature (using anti-ICAM-1) [51,210].

6. Conclusions

US-mediated drug delivery is a promising strategy to improve the way drugs are delivered to diseased cardiovascular tissue. Backed with sound experimental evidence, this method relies on the ability of US to focus mechanical energy on well-defined tissues to manipulate barrier properties, or actuate biochemical pathways leading to increased drug penetration into the cell or tissue of interest. Acoustic cavitation facilitates drug delivery through its mechanical effects and by releasing therapeutics from drug-loaded vesicles. Targeting

methods, such as radiation force and biomolecular ligands, localize drug-loaded vesicles near the endothelium for efficient delivery. Sonoporation has been demonstrated as a means of cellular therapeutic delivery through US-induced pores. Delivery to the vascular wall and beyond relies on permeabilization of the endothelium, which can be enhanced by paracellular transport, transcytosis or frank breach of the endothelial layer. Drug delivery to thrombus can be augmented by sonothrombolysis, which has been established as an effective method to recanalize cerebral vessels in clinical trials. The mechanisms of US-mediated drug delivery outlined in this review remain debated. However, future conclusions drawn from ongoing investigations will both add to the understanding of US-mediated cardiovascular drug delivery and improve the efficacy of treatments based on these concepts. The ability to provide localized efficacious treatment to vascular beds to reverse endothelial dysfunction, treat cardiomyopathy, or accelerate thrombolysis would markedly change the clinical approach to the treatment of cardiovascular disease and stroke.

7. Expert opinion

7.1 Challenges and gaps in knowledge

In the US-mediated drug delivery literature, there is a paucity of studies demonstrating drug transport from the lumen into medial tissue. In their studies of calcein delivery to porcine carotid tissue, Laing *et al.* demonstrated strong calcein delivery to smooth muscle tissue, however, the route of transport could not be determined due to the considerable presence of vasa vasorum within porcine carotid medial tissue [112]. Within these studies, drug penetration seems to have occurred through and between the endothelial cells of the vasa vasorum into smooth muscle cells, and not via direct penetration through luminal endothelium. The IEL likely obstructed this route, which, along with endothelium, is a significant barrier to drug transport [82]. The mechanical forces required to manipulate this vascular layer – rich in dense elastin fibers – may be vastly different than those exerted on the endothelium. The IEL is relatively impermeable even to water, except for small, sparsely distributed fenestrated pores on the order of 1 μm in diameter [211]. Future studies should investigate the specific mechanical interactions necessary to manipulate this barrier to increase the efficacy of US-mediated drug delivery.

Nitric oxide, a short-lived but potent vasodilator, likely mediates paracellular permeability [212] via mechanotransduction of shear stress along the endothelium. Caveolin-1, a protein abundant within plasma membrane clefts, is known to bind endothelial nitric oxide synthase (eNOS) under normal shear conditions. Conformational changes in these proteins induced by high shear stress could liberate eNOS, leading to considerable activation of nitric oxide, vasodilation and tight junction opening [213]. Depicted in Figure 2, US-enhanced, caveolin-1-mediated paracellular permeability is achieved due to activation of mechanosensitive caveolins in the vascular endothelium [214,215]. Alternatively, paracellular permeability has been shown to diminish after periods of increased shear stress due to fluid flow in bovine brain microvascular endothelial cells [216]. These recent data on paracellular drug transport emphasize the need for continued research into the mechanisms of US-mediated drug delivery.

Currently, the efficiency of drug encapsulation techniques may limit the extent to which US-mediated drug delivery can elicit beneficial bioeffects *in vivo*. One promising strategy using a PFP emulsion formulation encapsulated up to 300 μg/ml of doxorubicin drug, with an approximate 50% release profile once exposed to US (Table 1) [217]. This compares with the systemic pharmacodynamic doxorubicin concentration near 17 μg/ml [218]. Targeting approaches will likely increase drug concentration near tissues of interest. Nevertheless, future improvements in encapsulation techniques will augment US-mediated drug delivery substantially.

Variability in the local cellular environment and the temporal dynamics of cavitation make individual responses to drug delivery therapy a challenge. In their investigation of cellular sonoporation in flow fields, Park *et al.* observed significant reduction in drug delivery *in vitro* when cells were cultured under shear stress [219]. Throughout the human vasculature, cells are exposed to varying amounts of shear stress depending on pathology, patient age and cardiovascular health. *In vivo* cavitation activity is also difficult to control, in part due to the use of polydisperse microbubble populations [220], variability of acoustic pressure *in situ* and vascular characteristics [221,222]. Understanding the manner in which these factors affect the cellular and mechanical mechanisms of US-mediated drug delivery will be imperative to successful treatment of cardiovascular disease.

The exact mechanisms that promote enhanced dissolution of blood clots in the presence of US and microbubbles have yet to be elucidated. While sonothrombolysis investigators have largely discounted thermal mechanisms [189], fibrin degradation product removal, fibrinolytic drug or microbubble penetration due to microstreaming and acoustic radiation force have been proposed as contributing factors (Figure 5). The mechanical and biochemical properties of the occlusive thrombus may also contribute to the degree of US enhancement of lysis [187,223,224]. Further research in this area will continue to refine the acoustic parameters necessary to develop efficient imaging and therapeutic US systems for sonothrombolysis.

7.2 Future directions

Non-invasive strategies for US-triggered local therapeutic gas delivery for cerebral ischemic injury are being developed. Bioactive gases such as xenon and nitric oxide are promising neuroprotective agents [225] with minimal adverse effects due to rapid vascular scavenging by hemoglobin. The results of preliminary studies [226,227] suggest that xenon, once released from a vesicle, provides neuroprotection for ischemic brain tissue quite efficiently.

Given the wide array of interdisciplinary studies that will inform future US-mediated drug delivery research, from vascular biology to computational simulation of bubble dynamics, we expect the development of savvy techniques to facilitate successful clinical translation. For example, determination of optimal drug delivery schemes will spur a new US modality for theragnostic applications. Molecularly targeted, theragnostic agents are a low-cost, functional strategy to image the extent of disease using US with high spatial sensitivity and specificity prior to clinical therapeutic intervention. The ability to confirm disease status and trigger delivery of a therapeutic with the same agent would help ensure that only potentially responsive patients would be treated, which in turn would streamline clinical trials of these

agents. Patil *et al.* describe one such example to track flowing microbubbles accumulating along a vessel border with harmonic imaging [228]. In their study, three consecutive pulses (two inversion pulses, one radiation force pulse) were used to cancel linear tissue and bubble effects while 'pushing' microbubbles to the perimeter of the lumen. Their results revealed an optimum frequency range for microbubble radiation force, which can be harnessed for future investigations. Hitchcock *et al.* [72] and Goertz *et al.* [229] demonstrated that for a fixed treatment period, the 'cavitation dose' and thus beneficial bioeffect can be maximized by inserting quiescent periods in the US exposure. The quiescent periods were dependent on the vascular flow rate.

Real-time methods to monitor drug delivery are also under investigation. Magnetic resonance imaging (MRI) guidance has been critical to the clinical translation of US thermal ablation. It is expected that analogous advances will be made for US-mediated drug delivery. Passive cavitation imaging techniques have been developed to monitor microbubble-enhanced US thermal ablation [76,77,230]. These techniques have been applied to differentiate stable and inertial cavitation from contrast agents in flow [78,231]. Furthermore, the image quality has been shown to be independent of the US insonation parameters. The authors anticipate investigations to enhance and monitor drug delivery efficacy will increase in frequency as investigators continue to reveal the proficiency of US-mediated drug delivery in treating cardiovascular pathologies.

Acknowledgments

The authors would like to thank D Ruberg from the School of Design, Architecture, Arts, and Planning at the University of Cincinnati for his assistance with the graphical preparation of figures.

Bibliography

Papers of special note have been highlighted as either of interest (•) or of considerable interest (••) to readers.

1. Komarova Y, Malik A. Regulation of endothelial permeability via paracellular and transcellular transport pathways. Annu Rev Physiol. 2010; 72(1):463–93. [PubMed: 20148685]
2. Zaragoza C, Márquez S, Saura M. Endothelial mechanosensors of shear stress as regulators of atherogenesis. Curr Opin Lipidol. 2012; 23(5):446–52. [PubMed: 22964993]
3. Binsalamah Z, Paul A, Prakash S, Shum-Tim D. Nanomedicine in cardiovascular therapy: recent advancements. Expert Rev Cardiovasc Ther. 2012; 10(6):805–15. [PubMed: 22894635]
4. Roger V, Go A, Lloyd-Jones D, et al. Heart disease and stroke statistics –2012 update: a report from the American Heart Association. Circulation. 2012; 125(1):e2–e220. [PubMed: 22179539]
5. Stancu C, Toma L, Sima A. Dual role of lipoproteins in endothelial cell dysfunction in atherosclerosis. Cell Tissue Res. 2012; 349(2):433–46. [PubMed: 22592627]
6. Libby P, Okamoto Y, Rocha V, Folco E. Inflammation in atherosclerosis: transition from theory to practice. Circ J. 2010; 74(2):213–20. [PubMed: 20065609]
7. Labreuche J, Deplanque D, Touboul P, et al. Association between change in plasma triglyceride levels and risk of stroke and carotid atherosclerosis: systematic review and meta-regression analysis. Atherosclerosis. 2010; 212(1):9–15. [PubMed: 20457452]
8. Saric M, Kronzon I. Aortic atherosclerosis and embolic events. Curr Cardiol Rep. 2012; 14(3):342–9. [PubMed: 22437371]
9. Mitragotri S. Devices for overcoming biological barriers: the use of physical forces to disrupt the barriers. Adv Drug Deliv Rev. 2013; 65(1):100–3. [PubMed: 22960787]

10. Gómez-Guerrero C, Mallavia B, Egido J. Targeting inflammation in cardiovascular diseases. Still a neglected field? Cardiovasc Ther. 2012; 30(4):189–97.
11. Perampaladas K, Gori T, Parker JD. Rosiglitazone causes endothelial dysfunction in humans. J Cardiovasc Pharmacol Ther. 2012; 17(3):260–5. [PubMed: 22053074]
12. Abdelwahid E, Siminiak T, Guarita-Souza L, et al. Stem cell therapy in heart diseases: a review of selected new perspectives, practical considerations and clinical applications. Curr Cardiol Rev. 2011; 7(3):201–12. [PubMed: 22758618]
13. Bernkop-Schnürch A, Hoffer MH, Kafedjiiski K. Thiomers for oral delivery of hydrophilic macromolecular drugs. Expert Opin Drug Deliv. 2004; 1(1):87–98. [PubMed: 16296722]
14. Laing ST, McPherson D. Cardiovascular therapeutic uses of targeted ultrasound contrast agents. Cardiovasc Res. 2009; 83(4):626–35. [PubMed: 19581314]
15. Galagudza MM, Korolev DV, Sonin DL, et al. Passive and active target delivery of drugs to ischemic myocardium. Bull Exp Biol Med. 2011; 152(1):105–7. [PubMed: 22803053]
16. Chistiakov D, Sobenin I, Orekhov A. Strategies to deliver microRNAs as potential therapeutics in the treatment of cardiovascular pathology. Drug Deliv. 2012; 19(8):392–405. [PubMed: 23173580]
17. Park J, Zhang Y, Vykhodtseva N, et al. The kinetics of blood brain barrier permeability and targeted doxorubicin delivery into brain induced by focused ultrasound. J Control Release. 2012; 162(1):134–42. [PubMed: 22709590]
18. Huang SL, MacDonald RC. Acoustically active liposomes for drug encapsulation and ultrasound-triggered release. Biochim Biophys Acta. 2004; 1665(1–2):134–41. [PubMed: 15471579]
19. Ali MH, Schumacker PT. Endothelial responses to mechanical stress: where is the mechanosensor? Crit Care Med. 2002; 30(5):S198–206. [PubMed: 12004236]
20. Lindner JR. Molecular imaging with contrast ultrasound and targeted microbubbles. J Nucl Cardiol. 2004; 11(2):215–21. [PubMed: 15052252]
21. Liu Y, Miyoshi H, Nakamura M. Encapsulated ultrasound microbubbles: therapeutic application in drug/gene delivery. J Control Release. 2006; 114(1):89–99. [PubMed: 16824637]
22. Bekeredjian R, Grayburn PA, Shohet RV. Use of ultrasound contrast agents for gene or drug delivery in cardiovascular medicine. J Am Coll Cardiol. 2005; 45(3):329–35. [PubMed: 15680708]
23. Bull JL. The application of microbubbles for targeted drug delivery. Expert Opin Drug Deilv. 2007; 4(5):475–93.
24. Muzykantov VR. Biomedical aspects of targeted delivery of drugs to pulmonary endothelium. Expert Opin Drug Deliv. 2005; 2(5):909–26. [PubMed: 16296786]
25. Vestweber D. Adhesion and signaling molecules controlling the transmigration of leukocytes through endothelium. Immunol Rev. 2007; 218:178–96. [PubMed: 17624953]
26. Muzykantov VR, Radhakrishnan R, Eckmann DM. Dynamic factors controlling targeting nanocarriers to vascular endothelium. Curr Drug Metab. 2012; 13(1):70–81. [PubMed: 22292809]
27. Apfel RE. Acoustic cavitation prediction. J Acoust Soc Am. 1981; 69(6):1624–33.
28. Apfel RE. Acoustic cavitation: a possible consequence of biomedical uses of ultrasound. Br J Cancer Suppl. 1982; 45(5):140–6. [PubMed: 6950749]
29. Carstensen EL, Flynn HG. The potential for transient cavitation with microsecond pulses of ultrasound. Ultrasound Med Biol. 1982; 8(6):L720–4. [PubMed: 7164178]
30. Flynn HG. Generation of transient cavities in liquids by microsecond pulses of ultrasound. J Acoust Soc Am. 1982; 72(6):1926–32.
31. Flynn HG, Church CC. Mechanism for the generation of cavitation maxima by pulsed ultrasound. J Acoust Soc Am. 1984; 76(2):505–12. [PubMed: 6481000]
32. Atchley AA, Frizzell LA, Apfel RE, et al. Thresholds for cavitation produced in water by pulsed ultrasound. Ultrasonics. 1988; 26(5):280–5. [PubMed: 3407017]
33. Holland CK, Apfel RE. Improved theory for the prediction of microcavitation thresholds. IEEE T Ultrason Ferr. 1989; 36(2):204–8.
34. Holland CK, Apfel RE. Thresholds for transient cavitation produced by pulsed ultrasound in a controlled nuclei environment. J Acoust Soc Am. 1990; 88(5):2059–69. [PubMed: 2269722]

35. Apfel RE, Holland CK. Gauging the likelihood of cavitation from short-pulse, low duty cycle ultrasound. Ultrasound Med Biol. 1991; 17:179–85. [PubMed: 2053214]
36. Holland CK, Roy RA, Apfel RE, Crum LA. In vitro detection of cavitation induced by a diagnostic ultrasound system. IEEE T Ultrason Ferr. 1992; 39:95–101.
37. Holland CK, Deng CX, Apfel RE, et al. Direct evidence of cavitation in vivo from diagnostic ultrasound. Ultrasound Med Biol. 1996; 22(7):917–25. [PubMed: 8923710]
38. Deng CX, Xu Q, Apfel RE, Holland CK. In vitro measurements of inertial cavitation thresholds in human blood. Ultrasound Med Biol. 1996; 22(7):939–48. [PubMed: 8923712]
39. Deng CX, Xu Q, Apfel RE, Holland CK. Inertial cavitation produced by pulsed ultrasound in controlled host media. J Acoust Soc Am. 1996; 100(2 Pt 1):1199–208. [PubMed: 8759969]
40. Coussios C, Roy RA. Applications of acoustics and cavitation to noninvasive therapy and drug delivery. Annu Rev Fluid Mech. 2008; 40:395–420.
41. Bader K, Holland C. Gauging the likelihood of stable cavitation from ultrasound contrast agents. Phys Med Biol. 2013; 58:127–44. [PubMed: 23221109]
42. Flynn, H. Physics of acoustic cavitation in liquids. In: Mason, WP., editor. Physical Acoustics. Academic Press; New York: 1964. p. 58-172.
43. Phelps AD, Leighton TG. The subharmonic oscillations and combination-frequency subharmonic emissions from a resonant bubble: their properties and generation mechanisms. Acustica. 1997; 83(1):59–66.
44. Elder SA. Cavitation microstreaming. J Acoust Soc Am. 1958; 31:54–64.
45. Miller DL. Particle gathering and microstreaming near ultrasonically activated gas-filled micropores. J Acoust Soc Am. 1988; 84(4):1378–87. [PubMed: 3198872]
46. Crum LA. Cavitation microjets as a contributory mechanism for renal calculi disintegration in ESWL. J Urol. 1988; 140(6):1587–90. [PubMed: 3057239]
47. Bailey MR, Blackstock DT, Cleveland RO, Crum LA. Comparison of electrohydraulic lithotripters with rigid and pressure-release ellipsoidal reflectors. I. Acoustic fields. J Acoust Soc Am. 1998; 104(4):2517–24. [PubMed: 10491712]
48. Bailey MR, Blackstock DT, Cleveland RO, Crum LA. Comparison of electrohydraulic lithotripters with rigid and pressure-release ellipsoidal reflectors. II. Cavitation fields. J Acoust Soc Am. 1999; 106(2):1149–60. [PubMed: 10462818]
49. Asaka T, Marston P. Acoustic radiation force on a bubble driven above resonance. J Acoust Soc Am. 1994; (96):3096–9.
50. Rudenko O, Sarvaszyan A, Emelianov S. Acoustic radiation force and streaming induced by focused nonlinear ultrasound in a dissipative medium. J Acoust Soc Am. 1996; (99):2791–8.
51. Dayton P, Klibanov AL, Brandenburger G, Ferrara KW. Acoustic radiation force in vivo: a mechanism to assist targeting of microbubbles. Ultrasound Med Biol. 1999; 25(8):1195–201. [PubMed: 10576262]
52. Tartis MS, McCallan J, Lum AF, et al. Therapeutic effects of paclitaxel-containing ultrasound contrast agents. Ultrasound Med Biol. 2006; 32(11):1771–80. [PubMed: 17112963]
53. Nyborg, J. Acoustic streaming. In: Mason, WP., editor. Physical Acoustics. 2. Academic Press; New York: 1965. p. 266-331.
54. Wu J, Du G. Acoustic streaming generated by a focused gaussian beam and finite amplitude tonebursts. Ultrasound Med Biol. 1993; 19(2):167–76. [PubMed: 8516962]
55. Wu J, Nyborg WL. Ultrasound, cavitation bubbles and their interaction with cells. Adv Drug Deliv Rev. 2008; 60(10):1103–16. [PubMed: 18468716]
56. Newman C, Bettinger T. Gene therapy progress and prospects: ultrasound for gene transfer. Gene Ther. 2007; 14:465–75. [PubMed: 17339881]
57. Lawrie A, Brisken AF, Francis SE, et al. Ultrasound-enhanced transgene expression in vascular cells is not dependent upon cavitation-induced free radicals. Ultrasound Med Biol. 2003; 29(10): 1453–61. [PubMed: 14597342]
58. Unger EC, Hersh E, Vannan M, McCreery T. Gene delivery using ultrasound contrast agents. Echocardiography. 2001; 18(4):355–61. [PubMed: 11415509]

59. Bekeredjian R, Chen S, Frenkel PA, et al. Ultrasound-targeted microbubble destruction can repeatedly direct highly specific plasmid expression to the heart. Circulation. 2003; 108(8):1022–6. [PubMed: 12912823]
60. Kodama T, Tomita Y, Koshiyama K, Blomley MJ. Transfection effect of microbubbles on cells in superposed ultrasound waves and behavior of cavitation bubble. Ultrasound Med Biol. 2006; 32(6):905–14. [PubMed: 16785012]
61. Suzuki R, Takizawa T, Negishi Y, et al. Gene delivery by combination of novel liposomal bubbles with perfluoropropane and ultrasound. J Control Release. 2007; 117(1):130–6. [PubMed: 17113176]
62. Hernot S, Klibanov AL. Microbubbles in ultrasound-triggered drug and gene delivery. Adv Drug Deliv Rev. 2008; 60(10):1153–66. [PubMed: 18486268]
63. Suzuki J, Ogawa M, Takayama K, et al. Ultrasound-microbubble-mediated intercellular adhesion molecule-1 small interfering ribonucleic acid transfection attenuates neointimal formation after arterial injury in mice. J Am Coll Cardiol. 2010; 55(9):904–13. [PubMed: 20185042]
64. Chen H, Brayman A, Evan A, Matula T. Preliminary observations on the spatial correlation between short-burst microbubble oscillations and vascular bioeffects. Ultrasound Med Biol. 2012; 38(12):2151–62. [PubMed: 23069136]
65. Phillips LC, Klibanov AL, Wamhoff BR, Hossack JA. Intravascular ultrasound detection and delivery of molecularly targeted microbubbles for gene delivery. IEEE T Ultrason Ferr. 2012; 59(7):1596–601.
66. Everbach EC, Francis CW. Cavitational mechanisms in ultrasound-accelerated thrombolysis at 1 MHz. Ultrasound Med Biol. 2000; 26(7):1153–60. [PubMed: 11053750]
67. Datta S, Coussios CC, McAdory LE, et al. Correlation of cavitation with ultrasound enhancement of thrombolysis. Ultrasound Med Biol. 2006; 32(8):1257–67. [PubMed: 16875959]
68. Prokop AF, Soltani A, Roy RA. Cavitational mechanisms in ultrasound-accelerated fibrinolysis. Ultrasound Med Biol. 2007; 33(6):924–33. [PubMed: 17434661]
69. Datta S, Coussios C, Ammi AY, et al. Ultrasound-enhanced thrombolysis using Definity® as a cavitation nucleation agent. Ultrasound Med Biol. 2008; 34:1421–33. [PubMed: 18378380]
70. Hitchcock K, Ivancevich N, Haworth K, et al. Ultrasound-enhanced rt-PA thrombolysis in an ex vivo porcine carotid artery model. Ultrasound Med Biol. 2011; 37(8):1240–51. [PubMed: 21723448]
71. Roy RA, Madanshetty SI, Apfel RE. An acoustic backscattering technique for the detection of transient cavitation produced by microsecond pulses of ultrasound. J Acoust Soc Am. 1990; 87(6): 2451–8. [PubMed: 2373791]
72. Madanshetty SI, Roy RA, Apfel RE. Acoustic microcavitation: its active and passive acoustic detection. J Acoust Soc Am. 1991; 90(3):1515–26. [PubMed: 1939908]
73. Farny C, Holt RG, Roy RA. Temporal and spatial detection of HIFU-induced inertial and hot-vapor cavitation with a diagnostic ultrasound system. Ultrasound Med Biol. 2009; 35(4):603–15. [PubMed: 19110368]
74. Salgaonkar VA, Datta S, Holland C, Mast TD. Passive cavitation imaging with ultrasound arrays. J Acoust Soc Am. 2009; 126(6):3071–83. [PubMed: 20000921]
75. Gyongy M, Coussios C. Passive spatial mapping of inertial cavitation during HIFU exposure. IEEE T Bio-med Eng. 2010; 57(1):48–56.
76. Haworth K, Mast TD, Radhakrishnan K, et al. Passive imaging with pulsed ultrasound insonations. J Acoust Soc Am. 2012; 132(1):544–53. [PubMed: 22779500]
77. Shankar PM, Dala Krishna P, Newhouse VL. Advantages of subharmonic over second harmonic backscatter for contrast-to-tissue echo enhancement. Ultrasound Med Biol. 1998; 24(3):395–9. [PubMed: 9587994]
78. Krishna PD, Shankar PM, Newhouse VL. Subharmonic generation from ultrasonic contrast agents. Phys Med Biol. 1999; 44(3):681–94. [PubMed: 10211802]
79. Shi WT, Forsberg F, Hall AL, et al. Subharmonic imaging with microbubble contrast agents: initial results. Ultrason Imaging. 1999; 21(2):79–94. [PubMed: 10485563]
80. Tanswell P, Seifried E, Stang E, Krause J. Pharmacokinetics and hepatic catabolism of tissue-type plasminogen activator. Arzneimittelforschung. 1991; 41(12):1310–19. [PubMed: 1815534]

81. Feigen VL, Lawes CM, Bennett DA, Anderson CS. Stroke epidemiology: a review of population-based studies of incidence, prevalence, and case-fatality in the late 20th century. Lancet Neurol. 2003; 2:43–53. [PubMed: 12849300]

82•. Penn MS, Saidel GM, Chisolm GM. Relative significance of endothelium and internal elastic lamina in regulating the entry of macromolecules into arteries in vivo. Circ Res. 1994; 74(1):74–82. This study uses an analytical model backed by experimental evidence to identify the endothelium as the major barrier to transport of a model tracer into murine vascular tissue. [PubMed: 8261597]

83. Penn MS, Rangaswamy S, Saidel GM, Chisolm GM. Macromolecular transport in the arterial intima: comparison of chronic and acute injuries. Am J Phsiol. 1997; 272(4 Pt 2):H1560–70.

84. Ochoa CD, Stevens T. Studies on the cell biology of interendothelial cell gaps. Am J Physiol-Lung C. 2012; 302(3):L275–86.

85. Kleinegris MC, Ten Cate-Hoek A, Ten Cate H. Coagulation and the vessel wall in thrombosis and atherosclerosis. Pol Arch Med Wewn. 2012; 122(11):557–66. [PubMed: 23160102]

86. Hirase T, Node K. Endothelial dysfunction as a cellular mechanism for vascular failure. Am J Physiol-Heart C. 2012; 302(3):H499–505.

87. Montezano A, Touyz R. Reactive oxygen species and endothelial function - role of nitric oxide synthase uncoupling and NOX family nicotinamide adenine dinucleotide phosphate oxidases. Basic Clin Pharmacol Toxicol. 2011; 110(1):87–94. [PubMed: 21883939]

88. Heo K, Fujiwara K, Abe J. Disturbed-flow-mediated vascular reactive oxygen species induce endothelial dysfunction. Circ J. 2011; 75(12):2722–30. [PubMed: 22076424]

89. Weis SM, Cheresh DA. Tumor angiogenesis: molecular pathways and therapeutic targets. Nat Med. 2011; 17(11):1359–70. [PubMed: 22064426]

90. Luissint A, Artus C, Glacial F, et al. Tight junctions at the blood brain barrier: physiological architecture and disease-associated dysregulation. Fluids Barriers CNS. 2012; 9(1):23. [PubMed: 23140302]

91. Krol S. Challenges in drug delivery to the brain: nature is against us. J Control Release. 2012; 164(2):145–55. [PubMed: 22609350]

92. Di L, Rong H, Feng B. Demystifying brain penetration in central nervous system drug discovery. J Med Chem. 2012; 56(1):2–12. [PubMed: 23075026]

93. Kuruvilla L, Kartha CC. Molecular mechanisms in endothelial regulation of cardiac function. Mol Cell Biochem. 2003; 253(1–2):113–23. [PubMed: 14619961]

94. Weis SM. Vascular permeability in cardiovascular disease and cancer. Curr Opin Hematol. 2008; 15(3):243–9. [PubMed: 18391792]

95. Triggle C, Samuel S, Ravishankar S, et al. The endothelium: influencing vascular smooth muscle in many ways. Can J Physiol Pharmacol. 2012; 90(6):713–38. [PubMed: 22625870]

96. Curry F, Adamson R. Vascular permeability modulation at the cell, microvessel, or whole organ level: towards closing gaps in our knowledge. Cardiovasc Res. 2010; 87(2):218–29. [PubMed: 20418473]

97. Komaru T, Kanatsuka H, Shirato K. Coronary microcirculation: physiology and pharmacology. Pharmacol Ther. 2000; 86(3):217–61. [PubMed: 10882810]

98. Yeager M. Structure of cardiac gap junction intercellular channels. J Struct Biol. 1998; 121(2): 231–45. [PubMed: 9615440]

99. Jain RK, Carmeliet P. SnapShot: tumor angiogenesis. Cell. 2012; 149(6):1408–1408. e1. [PubMed: 22682256]

100. Carmeliet P, Jain R. Molecular mechanisms and clinical applications of angiogenesis. Nature. 2011; 473(7347):298–307. [PubMed: 21593862]

101. Kost J, Langer R. Magnetically modulated drug delivery systems. Pharm Inter. 1986; 7(3):60–3.

102. Raemdonck K, Demeester J, De Smedt S. Advanced nanogel engineering for drug delivery. Soft Matter. 2009; 5(4):707–15.

103. Uesugi Y, Kawata H, Jo J, et al. An ultrasound-responsive nano delivery system of tissue-type plasminogen activator for thrombolytic therapy. J Control Release. 2010; 147(2):269–77. [PubMed: 20696194]

104. Yokoyama M. Polymeric micelles as a new drug carrier system and their required considerations for clinical trials. Expert Opin Drug Deliv. 2010; 7(2):145–58. [PubMed: 20095939]

105. Kataoka K, Harada A, Nagasaki Y. Block copolymer micelles for drug delivery: design, characterization and biological significance. Adv Drug Deliv Rev. 2012; 47(1):113–131. [PubMed: 11251249]

106. Fabiilli ML, Haworth KJ, Sebastian IE, et al. Delivery of chlorambucil using an acoustically-triggered perfluoropentane emulsion. Ultrasound Med Biol. 2010; 36(8):1364–75. [PubMed: 20691925]

107. Fabiilli ML, Lee J, Kripfgans OD, et al. Delivery of water-soluble drugs using acoustically triggered perfluorocarbon double emulsions. Pharm Res. 2010; 27(12):2753–65. [PubMed: 20872050]

108. Rapoport N, Kennedy A, Shea J, et al. Controlled and targeted tumor chemotherapy by ultrasound-activated nanoemulsions/microbubbles. J Control Release. 2009; 138(3):268–76. [PubMed: 19477208]

109. Huang SL, Hamilton AJ, Pozharski E, et al. Physical correlates of the ultrasonic reflectivity of lipid dispersions suitable as diagnostic contrast agents. Ultrasound Med Biol. 2002; 28(3):339–48. [PubMed: 11978414]

110. Klegerman ME, Hamilton AJ, Huang SL, et al. Quantitative immunoblot assay for assessment of liposomal antibody conjugation efficiency. Anal Biochem. 2002; 300(1):46–52. [PubMed: 11743691]

111•. Huang S. Liposomes in ultrasonic drug and gene delivery. Adv Drug Deliv Rev. 2008; 60(10): 1167–76. This comprehensive review of echogenic liposomes outlines manufacturing strategies and potential applications of these novel US contrast agents. [PubMed: 18479776]

112••. Laing ST, Kim H, Kopechek JA, et al. Ultrasound-mediated delivery of echogenic immunoliposomes to porcine vascular smooth muscle cells in vivo. J Liposome Res. 2009; 20(10):160–7. Exposure of porcine carotid arteries *in vivo* to 1-MHz US resulted in calcein penetration into smooth muscle cells. [PubMed: 19842795]

113. Buchanan KD, Huang S, Kim H, et al. Encapsulation of NF-kappaB decoy oligonucleotides within echogenic liposomes and ultrasound-triggered release. J Control Release. 2010; 141(2): 193–8. [PubMed: 19804805]

114. Klegerman M, Wassler M, Huang S, et al. Liposomal modular complexes for simultaneous targeted delivery of bioactive gases and therapeutics. J Control Release. 2010; 142(3):326–31. [PubMed: 19903503]

115. Ferrara KW, Borden MA, Zhang H. Lipid-shelled vehicles: engineering for ultrasound molecular imaging and drug delivery. Acc Chem Res. 2009; 42(7):881–92. [PubMed: 19552457]

116. Kopechek JA, Abruzzo TM, Wang B, et al. Ultrasound-mediated release of hydrophilic and lipophilic agents from echogenic liposomes. J Ultrasound Med. 2008; 27(11):1597–606. [PubMed: 18946099]

117. Rapoport N. Ultrasound-mediated micellar drug delivery. Int J Hyperthermia. 2012; 28(4):374–85. [PubMed: 22621738]

118. Laza-Knoerr A, Gref R, Couvreur P. Cyclodextrins for drug delivery. J Drug Target. 2010; 18(9): 645–56. [PubMed: 20497090]

119. Pasut G, Veronese FM. State of the art in PEGylation: the great versatility achieved after forty years of research. J Control Release. 2012; 161(2):461–72. [PubMed: 22094104]

120. Schroeder A, Kost J, Barenholz Y. Ultrasound, liposomes, and drug delivery: principles for using ultrasound to control the release of drugs from liposomes. Chem Phys Lipids. 2009; 162(1–2):1–16. [PubMed: 19703435]

121. Needham D, Anyarambhatla G, Kong G, Dewhirst MW. A new temperature-sensitive liposome for use with mild hyperthermia: characterization and testing in a human tumor xenograft model. Cancer Res. 2000; 60(5):1197–201. [PubMed: 10728674]

122. Dromi S, Frenkel V, Luk A, et al. Pulsed-high intensity focused ultrasound and low temperature-sensitive liposomes for enhanced targeted drug delivery and antitumor effect. Clin Cancer Res. 2007; 13(9):2722–7. [PubMed: 17473205]

123. Kooiman K, Foppen-Harteveld M, Steen AF, Jong N. Sonoporation of endothelial cells by vibrating targeted microbubbles. J Control Release. 2011; 154(1):35–41. [PubMed: 21514333]

124. Fan Z, Liu H, Mayer M, Deng C. Spatiotemporally controlled single cell sonoporation. Proc Natl Acad Sci USA. 2012; 109(41):16486–91. [PubMed: 23012425]

125••. Francis CW, Blinc A, Lee S, Cox C. Ultrasound accelerates transport of recombinant tissue plasminogen activator into clots. Ultrasound Med Biol. 1995; 21(3):419–24. This flagship study on sonothrombolysis documents increased penetration of a fibrinolytic enzyme into blood clots in the presence of US. [PubMed: 7645133]

126. van Wamel A, Kooiman K, Harteveld M, et al. Vibrating microbubbles poking individual cells: drug transfer into cells via sonoporation. J Control Release. 2006; 112(2):149–55. [PubMed: 16556469]

127. Wagstaff KM, Jans DA. Nuclear drug delivery to target tumour cells. Eur J Pharmacol. 2009; 625(1–3):174–80. [PubMed: 19836384]

128. Rychak JJ, Lindner JR, Ley K, Klibanov AL. Deformable gas-filled microbubbles targeted to P-selectin. J Control Release. 2006; 114(3):288–99. [PubMed: 16887229]

129••. Sheikov N, McDannold N, Sharma S, Hynynen K. Effect of focused ultrasound applied with an ultrasound contrast agent on the tight junctional integrity of the brain microvascular endothelium. Ultrasound Med Biol. 2008; 34(7):1093–104. These authors exposed rats to 1.5-MHz US bursts to achieve temporary disruption of the BBB, and noted concurrent disintegration of tight junction signals. [PubMed: 18378064]

130. Juffermans L, Van Dijk A, Jongenelen C, et al. Ultrasound and microbubble-induced intra- and intercellular bioeffects in primary endothelial cells. Ultrasound Med Biol. 2009; 35(11):1917–27. [PubMed: 19766381]

131. Blinc A, Kennedy SD, Bryant RG, et al. Flow through clots determines the rate and pattern of fibrinolysis. Thromb Haemost. 1994; 71(2):230–5. [PubMed: 8191404]

132. Bajd F, Vidmar J, Blinc A, Sersa I. Microscopic clot fragment evidence of biochemo-mechanical degradation effects in thrombolysis. Thromb Res. 2010; 126(2):137–43. [PubMed: 20580981]

133•. Fan Z, Kumon R, Park J, Deng C. Intracellular delivery and calcium transients generated in sonoporation facilitated by microbubbles. J Control Release. 2009; 42(1):31–9. Uptake of dye into cardiomyoblast cells *in vitro* depends on their proximity to acoustically activated microbubbles. [PubMed: 19818371]

134. Bao S, Thrall BD, Miller DL. Transfection of a reporter plasmid into cultured cells by sonoporation in vitro. Ultrasound Med Biol. 1997; 23(6):953–9. [PubMed: 9300999]

135. Mehier-Humbert S, Bettinger T, Yan F, Guy RH. Plasma membrane poration induced by ultrasound exposure: implication for drug delivery. J Control Release. 2005; 104(1):213–22. [PubMed: 15866347]

136. Ward M, Wu J, Chiu JF. Experimental study of the effects of Optison concentration on sonoporation in vitro. Ultrasound Med Biol. 2000; 26(7):1169–75. [PubMed: 11053752]

137••. Zhou YT, Yang K, Cui J, et al. Controlled permeation of cell membrane by single bubble acoustic cavitation. J Control Release. 2012; 157(1):103–11. This study examines the bubble dynamics associated with membrane disruption as a result of sonoporation. [PubMed: 21945682]

138. Paul S, Katiyar A, Sarkar K, et al. Material characterization of the encapsulation of an ultrasound contrast microbubble and its subharmonic response: strain-softening interfacial elasticity model. J Acoust Soc Am. 2010; 127(6):3846–57. [PubMed: 20550283]

139. Overvelde M, Garbin V, Dollet B, et al. Dynamics of coated microbubbles adherent to a wall. Ultrasound Med Biol. 2011; 37(9):1500–8. [PubMed: 21816289]

140. Ilinskii YA, Zabolotskaya EA, Hay TA, Hamilton MF. Models of cylindrical bubble pulsation. J Acoust Soc Am. 2012; 132(3):1346–57. [PubMed: 22978863]

141. Ohl C, Arora M, Ikink R, et al. Sonoporation from jetting cavitation bubbles. Biophys J. 2006; 91(11):4285–95. [PubMed: 16950843]

142. Deng CX, Sieling F, Pan H, Cui J. Ultrasound-induced cell membrane porosity. Ultrasound Med Biol. 2004; 30(4):519–26. [PubMed: 15121254]

143••. Meijering B, Juffermans L, Van Wamel A, et al. Ultrasound and microbubble-targeted delivery of macromolecules is regulated by induction of endocytosis and pore formation. Circ Res. 2009;

104(5):679–87. Inhibition of endocytosis pathways decreases intracellular delivery of dextrans into endothelial cells *in vitro*. [PubMed: 19168443]

144. Pardridge WM. Brain drug targeting and gene technologies. Jpn J Pharmacol. 2001; 87(2):97–103. [PubMed: 11700018]
145. Zhou Y, Cui J, Deng C. Dynamics of sonoporation correlated with acoustic cavitation activities. Biophys J. 2008; 94(7):L51–3. [PubMed: 18212008]
146. Skyba DM, Kaul S. Advances in microbubble technology. Coron Artery Dis. 2000; 11:219.
147. Juffermans L, Dijkmans PA, Musters RJ, et al. Transient permeabilization of cell membranes by ultrasound-exposed microbubbles is related to formation of hydrogen peroxide. Am J Physiol-Heart C. 2006; 291(4):H1595–601.
148. Lionetti V, Fittipaldi A, Agostini S, et al. Enhanced caveolae-mediated endocytosis by diagnostic ultrasound in vitro. Ultrasound Med Biol. 2009; 35(1):136–43. [PubMed: 18950933]
149. Herbst SM, Klegerman ME, Kim H, et al. Delivery of stem cells to porcine arterial wall with echogenic liposomes conjugated to antibodies against CD34 and intercellular adhesion molecule-1. Mol Pharm. 2010; 7(1):3–11. [PubMed: 19719324]
150•. Hitchcock KE, Caudell DN, Sutton JT, et al. Ultrasound-enhanced delivery of targeted echogenic liposomes in a novel ex vivo mouse aorta model. J Control Release. 2010; 144(3): 288–93. Rhodamine dye conjugated to echogenic liposomes extravasated into murine aorta tissue only when exposed to 1-MHz US. [PubMed: 20202474]
151. Phillips LC, Klibanov AL, Warnhoff BR, Hossack JA. Intravascular ultrasound mediated delivery of DNA via microbubble carriers to an injured porcine artery in vivo. IEEE Ultrasonics Symposium. 2008; 1:1157.
152. Ho SY, Somerville J, Yip WC, Anderson RH. Transluminal balloon dilation of resected coarcted segments of thoracic aorta: histological study and clinical implications. Int J Cardiol. 1988; 19(1):99–105. [PubMed: 2967253]
153. Mukherjee D, Wong J, Griffin B, et al. Ten-fold augmentation of endothelial uptake of vascular endothelial growth factor with ultrasound after systemic administration. J Am Coll Cardiol. 2000; 35(6):1678–86. [PubMed: 10807476]
154. Chen S, Shohet RV, Bekeredjian R, et al. Optimization of ultrasound parameters for cardiac gene delivery of adenoviral or plasmid deoxyribonucleic acid by ultrasound-targeted microbubble destruction. J Am Coll Cardiol. 2003; 42(2):301–8. [PubMed: 12875768]
155. Bekeredjian R, Chen S, Grayburn PA, Shohet RV. Augmentation of cardiac protein delivery using ultrasound targeted microbubble destruction. Ultrasound Med Biol. 2005; 31(5):687–91. [PubMed: 15866418]
156. Choi JJ, Pernot M, Small SA, Konofagou EE. Noninvasive, transcranial and localized opening of the blood-brain barrier using focused ultrasound in mice. Ultrasound Med Biol. 2007; 33(1):95–104. [PubMed: 17189051]
157. Wible JH, Galen KP, Wojdyla JK, et al. Microbubbles induce renal hemorrhage when exposed to diagnostic ultrasound in anesthetized rats. Ultrasound Med Biol. 2002; 28(11–12):1535–46. [PubMed: 12498949]
158. Li T, Liu G, Li J, et al. Mechanisms of prostate permeability triggered by microbubble-mediated acoustic cavitation. Cell Biochem Biophys. 2012; 64(2):147–53. [PubMed: 22722876]
159. Price RJ, Skyba DM, Kaul S, Skalak TC. Delivery of colloidal particles and red blood cells to tissue through microvessel ruptures created by targeted microbubble destruction with ultrasound. Circulation. 1998; 98(13):1264–7. [PubMed: 9751673]
160. Chen H, Brayman AA, Kreider W, et al. Observations of translation and jetting of ultrasound-activated microbubbles in mesenteric microvessels. Ultrasound Med Biol. 2011; 37(12):2139–48. [PubMed: 22036639]
161. Allen JS, May DJ, Ferrara K. Dynamics of therapeutic ultrasound contrast agents. Ultrasound Med Biol. 2002; 28(6):805–16. [PubMed: 12113793]
162. Collis J, Manasseh R, Liovic P, et al. Cavitation microstreaming and stress fields created by microbubbles. Ultrasonics. 2010; 50(2):279.

163. Yang FY, Lin Y, Kang K, Chao T. Reversible blood-brain barrier disruption by repeated transcranial focused ultrasound allows enhanced extravasation. J Control Release. 2011; 150(1): 111–16. [PubMed: 21070825]

164. Mesiwala AH, Farrell L, Wenzel HJ, et al. High-intensity focused ultrasound selectively disrupts the blood-brain barrier in vivo. Ultrasound Med Biol. 2002; 28(3):389–400. [PubMed: 11978420]

165. McDannold N, Vykhodtseva N, Raymond S, et al. MRI-guided targeted blood-brain barrier disruption with focused ultrasound: histological findings in rabbits. Ultrasound Med Biol. 2005; 31(11):1527–37. [PubMed: 16286030]

166•. Vykhodtseva N, McDannold N, Hynynen K. Progress and problems in the application of focused ultrasound for blood-brain barrier disruption. Ultrasonics. 2008; 48:296. This review offers a discussion of specific obstacles in the development of effective strategies to deliver drugs across the BBB.

167. Jalali S, Huang Y, Dumont D, Hynynen K. Focused ultrasound-mediated BBB disruption is associated with an increase in activation of AKT: experimental study in rats. BMC Neurol. 2011; 10:114. [PubMed: 21078165]

168. Fanning AS, Mitic LL, Anderson JM. Transmembrane proteins in the tight junction barrier. J Am Soc Nephrol. 1999; 10(6):1337–45. [PubMed: 10361874]

169. Hopkins AM, Li D, Mrsny RJ, et al. Modulation of tight junction function by G protein-coupled events. Adv Drug Deliv Rev. 2000; 41(3):329–40. [PubMed: 10854690]

170. Pawson T. Assembly of cell regulatory systems through protein interaction domains. Science. 2003; 300(5618):445–52. [PubMed: 12702867]

171. Shang X, Wang P, Liu Y, et al. Mechanism of low-frequency ultrasound in opening blood–tumor barrier by tight junction. J Mol Neurosci. 2011; 43(3):364–9. [PubMed: 20852968]

172. Wood S, Anthony S, Brown R, et al. Effects of ultrasound and ultrasound contrast agent on vascular tissue. Cardiovasc Ultrasound. 2012; 10(1):29. [PubMed: 22805356]

173. Skyba D, Price R, Linka A, et al. Direct in vivo visualization of intravascular destruction of microbubbles by ultrasound and its local effects on tissue. Circulation. 1998; 98(4):290–3. [PubMed: 9711932]

174. Hwang JH, Brayman AA, Reidy MA, et al. Vascular effects induced by combined 1-MHz ultrasound and microbubble contrast agent treatments in vivo. Ultrasound Med Biol. 2005; 31(4): 553–64. [PubMed: 15831334]

175. Chen H, Brayman AA, Bailey MR, Matula TJ. Blood vessel rupture by cavitation. Urol Res. 2010; 38(4):321–6. [PubMed: 20680255]

176. Stieger SM, Caskey CF, Adamson RH, et al. Enhancement of vascular permeability with low-frequency contrast-enhanced ultrasound in chorioallantoic membrane model. Radiology. 2007; 243(1):112–21. [PubMed: 17392250]

177. Ghitescu L, Fixman A, Simionescu M, Simionescu N. Specific binding sites for albumin restricted to plasmalemmal vesicles of continuous capillary endothelium: receptor-mediated transcytosis. J Cell Biol. 1986; 102(4):1304–11. [PubMed: 3007533]

178. Yudina A, Moonen C. Ultrasound-induced cell permeabilisation and hyperthermia: strategies for local delivery of compounds with intracellular mode of action. Int J Hyperthermia. 2012; 28(4): 311–19. [PubMed: 22621733]

179. Palade GE, Bruns RR. Structural modulations of plasmalemmal vesicles. J Cell Biol. 1968; 37(3): 633–49. [PubMed: 11905197]

180. Niles WD, Malik AB. Endocytosis and exocytosis events regulate vesicle traffic in endothelial cells. J Membr Biol. 1999; 167(1):85–101. [PubMed: 9878078]

181. Schnitzer JE, Oh P, Pinney E, Allard J. Filipin-sensitive caveolae-mediated transport in endothelium: reduced transcytosis, scavenger endocytosis, and capillary permeability of select macromolecules. J Cell Biol. 1994; 127(5):1217–32. [PubMed: 7525606]

182. McIntosh DP, Tan XY, Oh P, Schnitzer JE. Targeting endothelium and its dynamic caveolae for tissue-specific transcytosis in vivo: a pathway to overcome cell barriers to drug and gene delivery. Proc Natl Acad Sci USA. 2002; 99(4):1996–2001. [PubMed: 11854497]

183. Alexandrov AV, Wojner AW, Grotta JC. CLOTBUST: design of a randomized trial of ultrasound-enhanced thrombolysis for acute ischemic stroke. J Neuroimaging. 2004; 14(2):108–12. [PubMed: 15095554]

184. Molina CA, Ribo M, Rubiera M, et al. Microbubble administration accelerates clot lysis during continuous 2-MHz ultrasound monitoring in stroke patients treated with intravenous tissue plasminogen activator. Stroke. 2006; 37(2):425–9. [PubMed: 16373632]

185. Holscher T, Wilkening WG, Molkenstruck S, et al. Transcranial sound field characterization. Ultrasound Med Biol. 2008; 34(6):980.

186. Molina CA, Montaner J, Arenillas JF, et al. Differential pattern of tissue plasminogen activator-induced proximal middle cerebral artery recanalization among stroke subtypes. Stroke. 2004; 35(2):486–90. [PubMed: 14707233]

187. Sutton J, Ivancevich N, Perrin S Jr, et al. Clot retraction affects the extent of ultrasound-enhanced thrombolysis in an ex vivo porcine thrombosis model. Ultrasound Med Biol. 2013 In press.

188. Dalkara T, Arsava EM. Can restoring incomplete microcirculatory reperfusion improve stroke outcome after thrombolysis? J Cereb Blood Flow Metab. 2012; 32(12):2091–9. [PubMed: 23047270]

189. Francis CW, Onundarson PT, Carstensen EL, et al. Enhancement of fibrinolysis in vitro by ultrasound. J Clin Invest. 1992; 90(5):2063–8. [PubMed: 1430229]

190. Blinc A, Francis CW, Trudnowski JL, Carstensen EL. Characterization of ultrasound-potentiated fibrinolysis in vitro. Blood. 1993; 81(10):2636–43. [PubMed: 8490172]

191. Tho P, Manasseh R, Ooi A. Cavitation microstreaming patterns in single and multiple bubble systems. J Fluid Mech. 2007; 576:191–223.

192. Hamilton AJ, Huang S, Warnick D, et al. Intravascular ultrasound molecular imaging of atheroma components in vivo. J Am Coll Cardiol. 2004; 43(3):460.

193. Villanueva FS, Jankowski RJ, Klibanov S, et al. Microbubbles targeted to intercellular adhesion molecule-1 bind to activated coronary artery endothelial cells. Circulation. 1998; 98(1):1–5. [PubMed: 9665051]

194. Kaufmann BA, Carr CL, Belcik JT, et al. Molecular imaging of the initial inflammatory response in atherosclerosis: implications for early detection of disease. Arterioscler Thromb Vasc Biol. 2010; 30(1):54–9. [PubMed: 19834105]

195. Tsutsui JM, Xie F, Cano M, et al. Detection of retained microbubbles in carotid arteries with real-time low mechanical index imaging in the setting of endothelial dysfunction. J Am Coll Cardiol. 2004; 44(5):1036–46. [PubMed: 15337216]

196. Weller GE, Villanueva F, Tom E, Wagner W. Targeted ultrasound contrast agents: in vitro assessment of endothelial dysfunction and multi-targeting to ICAM-1 and sialyl Lewisx. Biotechnol Bioeng. 2005; 92(6):780–8. [PubMed: 16121392]

197. Weller G, Villanueva FS, Klibanov AL, Wagner WR. Modulating targeted adhesion of an ultrasound contrast agent to dysfunctional endothelium. Ann Biomed Eng. 2002; 30(8):1019.

198. Takalkar, Am; Klibanov, AL.; Rychak, JJ., et al. Binding and detachment dynamics of microbubbles targeted to P-selectin under controlled shear flow. J Control Release. 2004; 96(3): 473–82. [PubMed: 15120903]

199. Ferrante E, Pickard J, Rychak J, et al. Dual targeting improves microbubble contrast agent adhesion to VCAM-1 and P-selectin under flow. J Control Release. 2009; 140(2):100–7. [PubMed: 19666063]

200. Culp WC, Porter TR, Lowery J, et al. Intracranial clot lysis with intravenous microbubbles and transcranial ultrasound in swine. Stroke. 2004; 35(10):2407–11. [PubMed: 15322299]

201. Xie F, Lof J, Matsunaga TO, et al. Diagnostic ultrasound combined with glycoprotein IIb/IIIa-targeted microbubbles improves microvascular recovery after acute coronary thrombotic occlusions. Circulation. 2009; 119(10):1378–85. [PubMed: 19255341]

202. Hua X, Liu P, Gao Y, et al. Construction of thrombus-targeted microbubbles carrying tissue plasminogen activator and their in vitro thrombolysis efficacy: a primary research. J Thromb Thrombolysis. 2010; 30(1):29–35. [PubMed: 20155435]

203. Alonso A, Dempfle C, Della Martina A, et al. In vivo clot lysis of human thrombus with intravenous abciximab immunobubbles and ultrasound. Thromb Res. 2009; 124(1):70–4. [PubMed: 19349068]

204. Unger EC, McCreery TP, Sweitzer RH, et al. In vitro studies of a new thrombus-specific ultrasound contrast agent. Am J Cardiol. 1998; 81(12):58G–61G.

205. Klegerman ME, Zou Y, McPherson DD. Fibrin-targeting of echogenic liposomes with inactivated tissue plasminogen activator. J Liposome Res. 2008; 18(2):95–112. [PubMed: 18569446]

206. Leong-Poi H, Song J, Rim SJ, et al. Influence of microbubble shell properties on ultrasound signals: implications for low-power perfusion imaging. J Am Soc Echocardiogr. 2002; 15:1276.

207. Behm CZ, Kaufmann BA, Carr C, et al. Molecular imaging of endothelial vascular cell adhesion molecule-1 expression and inflammatory cell recruitment during vasculogenesis and ischemia-mediated arteriogenesis. Circulation. 2008; 117(22):2902–11. [PubMed: 18506006]

208. Shortencarier MJ, Dayton PA, Bloch SH, et al. A method for radiation-force localized drug delivery using gas-filled lipospheres. IEEE T Ultrason Ferr. 2004; 51(7):822–31.

209. Rychak J, Klibanov AL, Hossack J. Acoustic radiation force enhances targeted delivery of ultrasound contrast microbubbles: in vitro verification. IEEE T Ultrason Ferr. 2005; 52(3):421–33.

210. Liu J, Zhang P, Liu P, et al. Endothelial adhesion of targeted microbubbles in both small and great vessels using ultrasound radiation force. Mol Imaging. 2012; 11(1):58–66. [PubMed: 22418028]

211. Tada S, Tarbell JM. Fenestral pore size in the internal elastic lamina affects transmural flow distribution in the artery wall. Ann Biomed Eng. 2001; 29(6):456–66. [PubMed: 11459339]

212•. VanBavel E. Effects of shear stress on endothelial cells: possible relevance for ultrasound applications. Prog Biophys Mol Biol. 2007; 93(1–3):374–83. This review discusses bioeffects induced by shear stress on the vascular endothelium induced by oscillating microbubbles. [PubMed: 16970981]

213. Yu J. Direct evidence for the role of caveolin-1 and caveolae in mechanotransduction and remodeling of blood vessels. J Clin Invest. 2006; 116(5):1284–91. [PubMed: 16670769]

214. Yang B, Radel C, Hughes D, et al. p190 RhoGTPase-activating protein links the beta1 integrin/caveolin-1 mechanosignaling complex to RhoA and actin remodeling. Arterioscler Thromb Vasc Biol. 2011; 31(2):376–83. [PubMed: 21051664]

215. Deng J, Huang Q, Wang F, et al. The role of caveolin-1 in Blood-brain barrier disruption induced by focused ultrasound combined with microbubbles. J Mol Neurosci. 2012; 46(3):677–87. [PubMed: 21861133]

216. Walsh T, Murphy R, Fitzpatrick P, et al. Stabilization of brain microvascular endothelial barrier function by shear stress involves VE-cadherin signaling leading to modulation of pTyroccludin levels. J Cell Physiol. 2011; 226(11):3053–63. [PubMed: 21302304]

217. Wang C, Kang S, Lee Y, et al. Aptamer-conjugated and drug-loaded acoustic droplets for ultrasound theranosis. Biomaterials. 2012; 33(6):1939–47. [PubMed: 22142768]

218. Kontny NE, Boos J, Würthwein G, et al. Minimization of the preanalytical error in pharmacokinetic analyses and therapeutic drug monitoring: focus on IV drug administration. Ther Drug Monit. 2012; 34(4):460–6. [PubMed: 22660605]

219. Park J, Fan Z, Deng C. Effects of shear stress cultivation on cell membrane disruption and intracellular calcium concentration in sonoporation of endothelial cells. J Biomech. 2011; 44(1):164–9. [PubMed: 20863503]

220. Stride E, Edirisinghe M. Novel preparation techniques for controlling microbubble uniformity: a comparison. Med Biol Eng. 2009; 47(8):892.

221. Qin S, Ferrara K. Acoustic response of compliable microvessels containing ultrasound contrast agents. Phys Med Biol. 2006; 51(20):5065–88. [PubMed: 17019026]

222. Qin S, Ferrara K. A model for the dynamics of ultrasound contrast agents in vivo. J Acoust Soc Am. 2010; 128(3):1511–21. [PubMed: 20815486]

223. Molina CA. Imaging the clot: does clot appearance predict the efficacy of thrombolysis? Stroke. 2005; 36(11):2333–4. [PubMed: 16224076]

224. Xie F, Everbach EC, Gao S, et al. Effects of attenuation and thrombus age on the success of ultrasound and microbubble-mediated thrombus dissolution. Ultrasound Med Biol. 2011; 37(2): 280–8. [PubMed: 21208727]

225. Eltzschig HK, Eckle T. Ischemia and reperfusion–from mechanism to translation. Nat Med. 2011; 17(11):1391–401. [PubMed: 22064429]

226. Derwall M, Coburn M, Rex S, et al. Xenon: recent developments and future perspectives. Minerva Anestesiol. 2009; 75(1–2):37–45. [PubMed: 18475253]

227. Britton GL, Kim H, Kee P, et al. In vivo therapeutic gas delivery for neuroprotection with echogenic liposomes. Circulation. 2010; 122(16):1578–87. [PubMed: 20921443]

228. Patil AV, Rychak JJ, Allen JS, et al. Dual frequency method for simultaneous translation and real-time imaging of ultrasound contrast agents within large blood vessels. Ultrasound Med Biol. 2009; 35(12):2021–30. [PubMed: 19828229]

229. Goertz D, Wright C, Hynynen K. Contrast agent kinetics in the rabbit brain during exposure to therapeutic ultrasound. Ultrasound Med Biol. 2010; 36(6):916–24. [PubMed: 20447757]

230. Jensen CR, Ritchie RW, Gyöngy M, et al. Spatiotemporal monitoring of high-intensity focused ultrasound therapy with passive acoustic mapping. Radiology. 2012; 262(1):252–61. [PubMed: 22025731]

231. Choi J, Coussios C. Spatiotemporal evolution of cavitation dynamics exhibited by flowing microbubbles during ultrasound exposure. J Acoust Soc Am. 2012; 132(5):3538–49. [PubMed: 23145633]

232. Kee PH, Abruzzo TA, Smith DA, et al. Synthesis, acoustic stability, and pharmacologic activities of papaverine-loaded echogenic liposomes for ultrasound controlled drug delivery. J Liposome Res. 2008; 18(4):263–77. [PubMed: 18720194]

233. Buchanan KD, Huang S, Kim H, et al. Encapsulation of NF-kappaB decoy oligonucleotides within echogenic liposomes and ultrasound-triggered release. J Control Release. 2009; 141(2): 193–8. [PubMed: 19804805]

234. Rothdiener M, Müller D, Castro P, et al. Targeted delivery of siRNA to CD33-positive tumor cells with liposomal carrier systems. J Control Release. 2010; 144(2):251–8. [PubMed: 20184933]

235. Huang S, Kee PH, Kim H, et al. Nitric oxide-loaded echogenic liposomes for nitric oxide delivery and inhibition of intimal hyperplasia. J Am Coll Cardiol. 2009; 54(7):659.

236. Smith D, Vaidya S, Kopechek J, et al. Ultrasound-triggered release of recombinant tissue-type plasminogen activator from echogenic liposomes. Ultrasound Med Biol. 2010; 36(1):145–57. [PubMed: 19900755]

237. Wang C, Yang C, Lin Y, et al. Anti-inflammatory effect with high intensity focused ultrasound-mediated pulsatile delivery of diclofenac. Biomaterials. 2012; 33(5):1547–53. [PubMed: 22082618]

238. Wang C, Kang S, Lee Y, et al. Aptamer-conjugated and drug-loaded acoustic droplets for ultrasound theranosis. Biomaterials. 2012; 33(6):1939–47. [PubMed: 22142768]

239. Jin H, Tan H, Zhao L, et al. Ultrasound-triggered thrombolysis using urokinase-loaded nanogels. Int J Pharm. 2012; 434(1–2):384–90. [PubMed: 22683455]

240. Liu J, Lewis TN, Prausnitz MR, Shohet RV. Non-invasive assessment and control of ultrasound-mediated membrane permeabilization. Pharm Res. 1998; 15(6):918–24. [PubMed: 9647359]

241. Kassell NF, Helm G, Simmons N, et al. Treatment of cerebral vasospasm with intra-arterial papaverine. J Neurosurg. 1992; 77(6):848–52. [PubMed: 1432125]

242. Giannoukakis N, Bonham CA, Qian S, et al. Prolongation of cardiac allograft survival using dendritic cells treated with NF-kB decoy oligodeoxyribonucleotides. Mol Ther. 2000; 1(5):430–7. [PubMed: 10933964]

243. Jang YL, Yun UJ, Lee MS, et al. Cell-penetrating peptide mimicking polymer-based combined delivery of paclitaxel and siRNA for enhanced tumor growth suppression. Int J Pharm. 2012; 434:488–93. [PubMed: 22613208]

244. Knauf WU, Lissichkov T, Aldaoud A, et al. Phase III randomized study of bendamustine compared with chlorambucil in previously untreated patients with chronic lymphocytic leukemia. J Clin Oncol. 2009; 27(26):4378–84. [PubMed: 19652068]

245. Gaffney PJ, Edgell TA. The international and “NIH” units for thrombin – how do they compare? Thromb Haemostasis. 1995; 74(3):900–3. [PubMed: 8571318]

246. Vanin AF, Timoshin AA. Determination of in vivo nitric oxide levels in animal tissues using a novel spin trapping technology. Nitric Oxide Methods Protocols. 2011; 704:135–49.

247. Wilhelm S, Ma D, Maze M. Effects of xenon on in vitro and in vivo models of neuronal injury. Anesthesiology. 2002; 96(6):1485–91. [PubMed: 12170064]

248. Shaw GJ, Meunier JM, Lindsell CJ, et al. Making the right choice: optimizing rt-PA and eptifibatide lysis, and in vitro study. Thromb Res. 2010; 126(4):e305–11. [PubMed: 20813398]

249. Lötsch J, Kettenmann B, Renner B, et al. Population pharmacokinetics of fast release oral diclofenac in healthy volunteers: relation to pharmacodynamics in an experimental pain model. Pharm Res. 2000; 17(1):77–84. [PubMed: 10714612]

250. Morris J, Dobson J. IV. Protocols for administration of doxorubicin and cisplatin. Small Animal Oncol. 2008:285.

251. del Zoppo GJ, Higashida RT, Furlan AJ, et al. PROACT: a phase II randomized trial of recombinant prourokinase by direct arterial delivery in acute middle cerebral artery. Stroke. 1998; 29(1):4–11. [PubMed: 9445320]

Article highlights

- Developments in ultrasound (US) technology and theragnostic agents have fostered a new method to administer therapeutics within the cardiovasculature: US-mediated drug delivery.
- Acoustically responsive vesicles capable of encapsulating and shielding targeted therapeutics from vascular degradation are being developed to increase the efficacy and scope of US-mediated drug delivery.
- Through their interaction with tissue, acoustically activated microbubbles can manipulate the barrier properties of vascular tissue by i) mechanically forming pores within the membranes of cells, ii) increasing transcellular or paracellular permeability of the endothelium and iii) targeting encapsulated therapeutics to the endothelial surface via acoustic radiation force.
- Sonothrombolysis is an established method of US-mediated drug delivery *in vitro* and *ex vivo*, and is currently under clinical investigation.
- Modalities combining therapeutic and diagnostic US are currently under development, which couple the benefits of US-mediated drug delivery with the diagnostic capabilities of traditional US technology.

This box summarizes key points contained in the article.

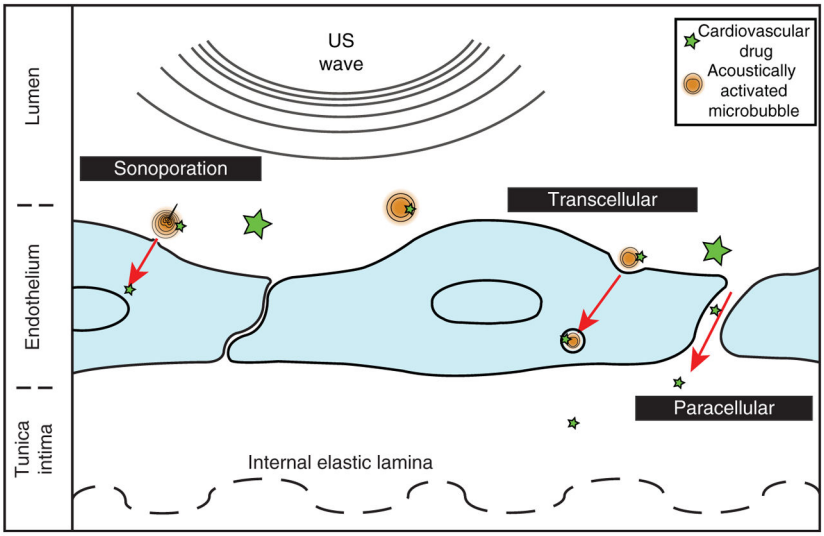

Figure 1. An overview of three penetration routes stimulated for ultrasound-mediated drug delivery

Sonoporation refers to the localized, mechanical disruption of a plasma membrane, which allows drugs and ions to diffuse passively. Transcellular pathways, such as endocytosis, involve active transport of drug via cytosolic vesicles. The paracellular route occurs when endothelial cells spread apart, either due to desquamation or by tight junction breakdown from bubble-induced shear stress.

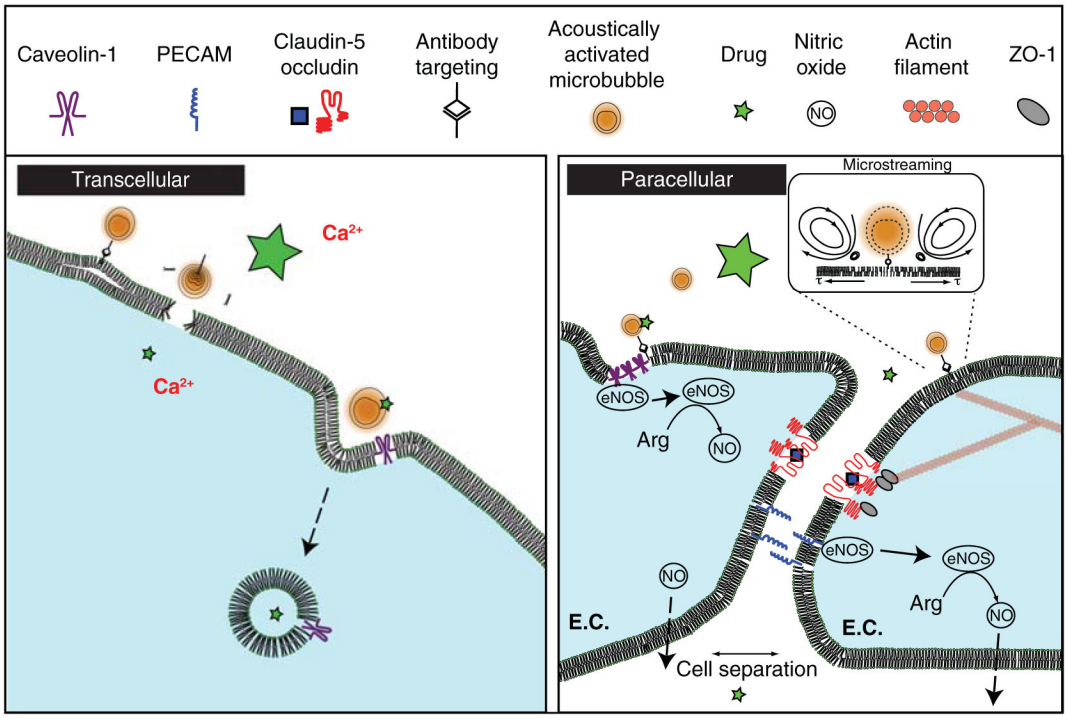

Figure 2. An overview of some proposed mechanisms for transcellular and paracellular ultrasound-mediated drug delivery

Transcellular: as a result of bubble-induced shear stress along the cell membrane, extracellular drugs can undergo caveolin-1-mediated endocytosis. Additionally, sonoporation can create ‘holes’ in the cell membrane facilitating influx of ions or drugs. Paracellular: shear stress from cavitation-induced microstreaming can cause caveolin-1 to detach from endothelial nitric oxide synthase (eNOS). Here, it converts arginine to nitric oxide, stimulating vasodilation and possible paracellular permeability. Alternatively, this shear stress deforms the actin cytoskeleton, which can cause conformational changes and breakdown of tight junction proteins (ZO-1, occludin).

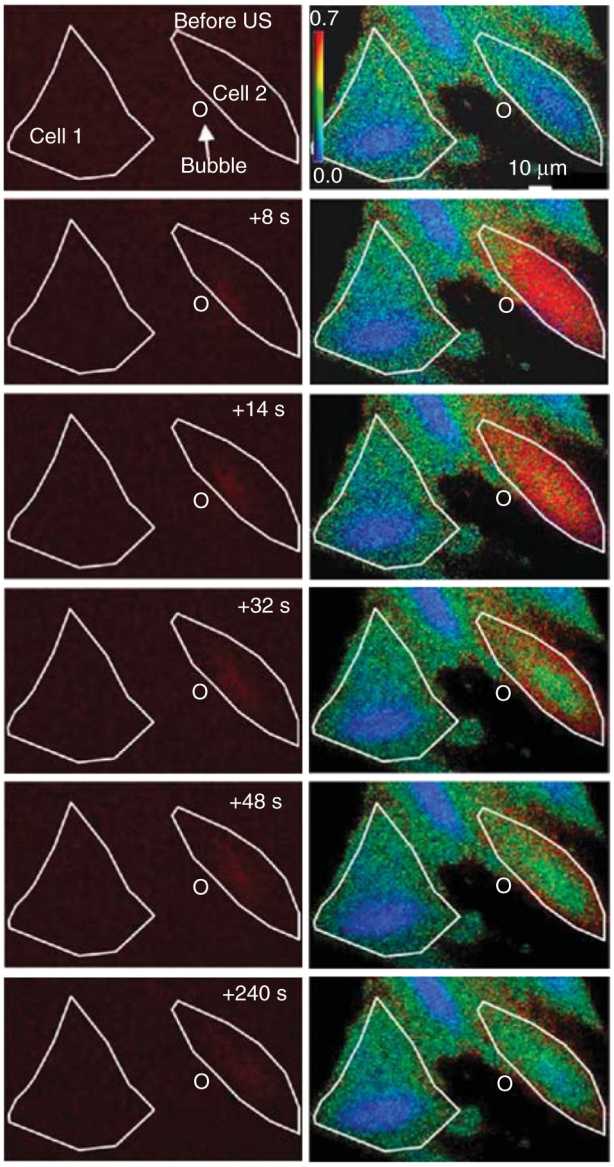

Figure 3. Propidium iodide (PI; left column) and intracellular $[Ca^{2+}]_i$ flux (right column) during microbubble oscillation near a cell membrane

Cell outlines, indicated by white lines, demarcate PI and Ca^{2+} delivery, when a bubble (circle) oscillates near its cell membrane. The initial state of the cell is seen in the first row, followed by subsequent images during ultrasound exposure.

Reprinted from Fan *et al.* [133], with permission from Elsevier (2012).

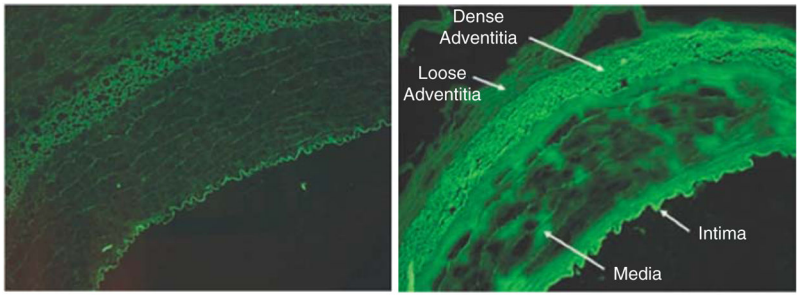

Figure 4. Images of calcein fluorescence indicating penetration of liposomes targeting to smooth muscle actin, in the absence (left) and presence (right) of ultrasound

Reprinted from Laing *et al.* [112], with permission from Informa Healthcare (2012).

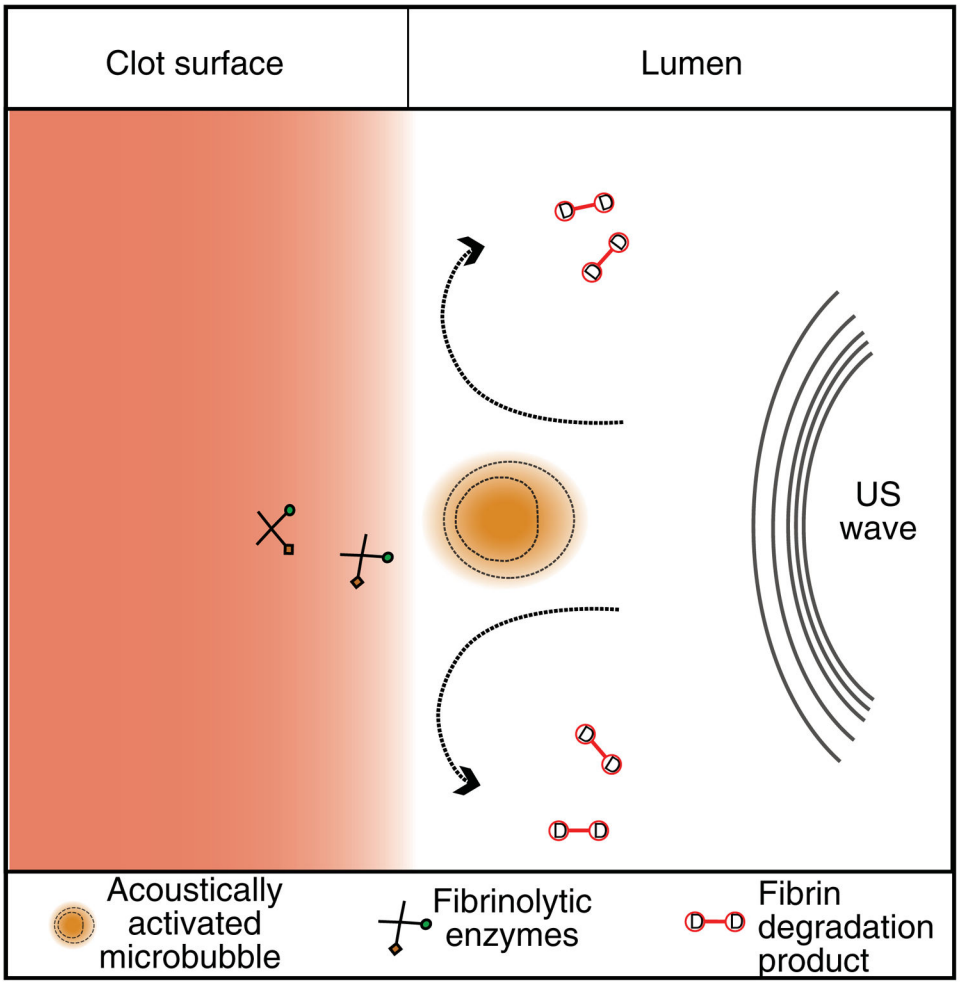

Figure 5. Cavitational mechanisms in sonothrombolysis

As a result of local fluid dynamics around a cavitating microbubbles, the fibrinolytic enzymes (recombinant tissue-plasminogen activator (rt-PA) and plasminogen) penetrate deeper into the fibrin matrix. Additionally, fluid microstreaming removes fibrin degradation products from the surface of the clot, expediting the fibrinolytic process.

Table 1

Comparison of drug vehicles.

Authors	Vehicle	Drug	Vehicle concentration	Drug concentration during systemic therapy
Kee *et al.* [232]	Liposome	Papaverine	1.85 mg/ml	3 mg/ml [241]
Buchanan *et al.* [113]	Liposome	NF-κB	2 mM	10 mM [242]
Rothdiener *et al.* [234]	Liposome	siRNA	500 mmole/mole lipid	2.7 mM [243]
Fabiilli *et al.* [106]	PFP droplet	Chlorambucil	3.12 mg/ml	0.02 mg/ml [244]
Fabiilli *et al.* [107]	PFP droplet	Thrombin	3.1 IU/ml	1.3 IU/ml [245]
Huang *et al.* [235]	Liposome	Nitric oxide	0.045 mM	1 mM [246]
Britton *et al.* [227]	Liposome	Xenon	150 μl/ml	3.2 mM [247]
Smith *et al.* [236]	Liposome	rt-PA	40 μg/mg lipid	2.8 μg/ml [248]
Wang *et al.* [237]	Alginate	Diclofenac	7.5 mg/ml	2.05 mg/ml [249]
Wang *et al.* [238]	PFP droplet	Doxorubicin	304 mg/ml	1.8 mg/ml [250]
Jin *et al.* [239]	Nanogel	Urokinase	500 mg/ml	4 mg/ml [251]

Therapeutic concentrations calculated by assuming average human weight and blood volume.

NF-κB: Nuclear factor-kappaB; PFP: Perfluoropentane; rt-PA: Recombinant tissue-plasminogen activator; siRNA: Small interfering RNA.

Table 2

Investigations of US-mediated drug delivery to cardiovascular tissue.

Authors	Tissue target	Vehicle	US exposure parameters	Bioeffect
Mehier-Humbert *et al.* [135]	*In vitro*; rat mammary	Perflutren liposomes	1.15 MHz, 0.42 MPa, 20% DC	Penetration of dextrans < 464 kDa
Liu *et al.* [240]	*In vitro*; bovine RBCs	None	24 kHz	Hemolysis correlated with $f_{1/2}$ emissions
Skyba *et al.* [173]	*In vivo*; rat spinotrapezius	Optison™	Short pulse, 2.3 MHz, P_r = 0.61 MPa_r	Capillary rupture
Mukherjee *et al.* [153]	*In vivo*; rat myocardium	Dextrose-albumin, perfluorocarbon	1 MHz; 0.33 MPa_r; 15 min	8 × VEGF uptake by endothelium
Ward *et al.* [136]	*In vitro*; Jurkat lymphocytes	Optison™	2 MHz, P_p = 0.2 MPa, 10% DC	Lethal sonoporation when bubble near cell membrane
Chen *et al.* [155]	*In vivo*; rat myocardium	Lipid-shelled, perfluoropropane	1.3 – 12 MHz; MI = 1.6; four cycles; ECG-gated	Increased delivery of viral and plasmid transgenes with US optimization
Lawrie *et al.* [57]	*In vitro*; porcine medial VSMCs	Optison™	956 kHz; P_r = 1.96 MPa_r	Free-radical independent luciferase expression
Bekeredjian *et al.* [22]	*In vivo*; rat heart	Lipid-shelled, octafluoropropane	1.3 MHz, MI = 1.5; four cycles; ECG-gated	Increased luciferase expression in heart tissue
Culp *et al.* [200]	*In vivo*; porcine rete mirabele	Eptifibitide albumin MBs	1 MHz; 2 W/cm^2	Recanalization in 6/8 occluded pigs
Datta *et al.* [69]	*In vitro*; porcine blood clot	Definity®	120 kHz, $P_{pk\text{-}pk}$ = 0.32 MPa 80% DC	Penetration of fibrinolytics into clot; clot mass loss enhancement
Phillips *et al.* [151]	*In vitro*; porcine coronary	Plasmid MBs	5 MHz; 2 MPa	6.5 × increase in transgene expression with MB + US
Meijering *et al.* [143]	*In vitro*; bovine aortic endothelium	Sonovue®	1 MHz, P_r = 0.22 MPa_r	Endocytotic transport of dextrans with MB + US
Hitchcock *et al.* [150].	*ex vivo*; murine aorta	Anti-ICAM – ELIP	1 MHz, CW, 0.49 $MPa_{pk\text{-}pk}$	ELIP penetration into tunica media
Laing *et al.* [112]	*In vivo*; porcine carotid	Anti-Actin – ELIP	1 MHz, CW, 0.23 $MPa_{pk\text{-}pk}$	ELIP penetration into tunica media
Herbst *et al.* [149]	*Ex vivo*; porcine aorta	Anti-ICAM – ELIP	1 MHz, CW, 0.15 $MPa_{pk\text{-}pk}$	ELIP penetration into tunica intima
Fan *et al.* [133]	*In vitro*; rat cardiomyoblast	Definity®	1 MHz, P_r = 0.27 MPa_r	Dye delivery in cells with adjacent MBs
Phillips *et al.* [151]	*In vivo*; rat carotid	Rapamycin MBs	1.2 MHz, CW, 0.14 MPa 5 MHz, 1.5 MPa	10% dose required for neointima reduction with MB + US
Liu *et al.* [21,210,240]	*In vitro*; mouse endothelium	AntiCD34-Zhifuxian	Long pulse, 1.1 MHz, 0.07 MPa	Endothelial targeting

CW: Continuous wave; DC: Duty cycle; ELIP: Echogenic immunoliposomes; ICAM: Intracellular adhesion molecule; MB: Microbubble; MI: Mechanical index; Pp: Peak positive acoustic pressure; $P_{pk\text{-}pk}$: Peak-to-peak acoustic pressure; P_r: Peak rarefactional acoustic pressure; RBC: Red blood cell; US: Ultrasound; VSMC: Vascular smooth muscle cell.